

Supporting Information

High Activity Cobalt Catalysts for Alkene Hydroboration with Electronically Responsive Terpyridine and α -Diimine Ligands.

*W. Neil Palmer, Tianning Diao, Iraklis Pappas and Paul J. Chirik**

Department of Chemistry, Frick Laboratory

Princeton University, Princeton, NJ 08544, USA

**Corresponding author's e-mail address: pchirik@princeton.edu*

Table of Contents

General Considerations	S2
Preparation of Cobalt Complexes	S4
Procedures for Catalytic Hydroboration and Pyridine Exchange	S9
Characterization of Hydroboration Products	S11
Additional Structures and Spectroscopic Data	S19
References	S35

I. General Considerations. All air- and moisture-sensitive manipulations were carried out using vacuum line, Schlenk and cannula techniques or in an MBraun inert atmosphere (nitrogen) dry box. All glassware was stored in a pre-heated oven prior to use. The solvents used in the dry box were dried and deoxygenated using literature procedures.¹ Deuterated solvents (Cambridge Isotope Laboratories) and HBPIn (Aldrich) were used without further purification. Solid olefins were dried under reduced pressure prior to use. Liquid olefins were dried on CaH₂ or LiAlH₄ and distilled under reduced pressure prior to use. The following compounds were prepared according to literature procedures: 4-(pyrrolidinyl)-(^{Mes}PDI)CoMe,² ⁱPrDI,³ (Py)₄CoCl₂,⁴ (Py)₂Co(CH₂SiMe₃)₂,⁴ isopropenylcyclohexane,⁵ and 1,1-dicyclohexylethylene.⁵

¹H NMR spectra were recorded on either Bruker 300 or 500 spectrophotometers operating at 300 MHz, and 500 MHz, respectively, or a Varian 400 spectrophotometer operating at 400 MHz. ¹³C NMR spectra were recorded on a Bruker 500 spectrometer operating at 126 MHz. All ¹H and ¹³C NMR chemical shifts are reported relative to SiMe₄ using the ¹H (residual) and ¹³C chemical shifts of the solvent as a secondary standard. The NMR spectra of all the hydroboration products were taken using CDCl₃ as the solvent unless otherwise specified. Carbons that are directly attached to boron atoms were not observed due to quadrupolar relaxation.⁶ The composition of product mixtures was determined by integration of characteristic peaks in the ¹H NMR or the quantitative ¹³C NMR spectra. ¹H NMR spectra of diastereomeric products were not assigned because their NMR resonances overlap with each other. Only their ¹³C NMR spectra were assigned.

Elemental analyses were performed at Robinson Microlit Laboratories, Inc., in Ledgewood, NJ. GC analyses were performed using a Shimadzu GC-2010 gas chromatograph equipped with a Shimadzu AOC-20s autosampler and a Shimadzu SHRXI-5MS capillary column (15m x 250 μ m). The instrument was set to an injection volume of 1 μ L, an inlet split ratio of 20:1, and inlet and detector temperatures of 250 °C and 275 °C, respectively. UHP-grade S3 helium was used as carrier gas with a flow rate of 1.82 mL/min. The temperature program used for all the analyses is as follows: 60 °C, 1 min; 15 °C/min to 250 °C, 2 minutes.

All DFT calculations were performed with the ORCA program package.⁷ The geometry optimizations of the complexes and single-point calculations on the optimized geometries were carried out at the B3LYP level of DFT.⁸ The all-electron Gaussian basis sets were those developed by Ahlrichs' group.⁹ Triple- ζ quality basis sets def2-TZVP with one set of polarization functions on the metals and on the atoms directly coordinated to the metal center were used. For the carbon and hydrogen atoms, slightly smaller polarized split-valence def2-SV(P) basis sets were used that were of double- ζ quality in the valence region and contained a polarizing set of d functions on the non-hydrogen atoms. Auxiliary basis sets were chosen to match the orbital basis.¹⁰ The RIJCOSX¹¹ approximation was used to accelerate the calculations.

Throughout this manuscript, computational results are described using the broken symmetry approach by Ginsberg¹² and Noodleman et al.¹³ Because several broken symmetry solutions to the spin-unrestricted Kohn-Sham equations may be obtained, the general notation broken symmetry (m,n)¹⁴ has been adopted, where m (n) denotes the number of spin-up (spin-down) electrons at the two interacting fragments.

Canonical and corresponding¹⁵ orbitals, as well as spin density plots, were generated with the program *Chimera*.¹⁶

II. Preparation of Cobalt Complexes

Preparation of (terpy)CoCH₂SiMe₃ (2). A 20 mL scintillation vial was charged with 0.424 g (1.083 mmol) of (py)₂Co(CH₂SiMe₃)₂³ and 10 mL of diethyl ether. While stirring, 0.253 g (1.083 mmol) 2,2';6',2"-terpyridine (terpy) was added and the resulting solution was allowed to stir at room temperature for 16 hours, during which time a color change from deep green to purple was observed. The solution was filtered through Celite and concentrated in vacuo. The resulting residue was recrystallized from pentane to yield 0.329 g (80%) of (terpy)Co(CH₂SiMe₃) as purple crystals. Anal Calcd for C₁₉H₂₂CoN₃Si: C, 60.15; H, 5.84; N, 11.07. Found: C, 59.72; H, 5.76; N, 10.91. ¹H NMR (500 MHz, benzene-*d*₆, 23 °C) δ 12.21 (d, *J*_{HH} = 5.9 Hz, 2H, 6,6" C-H), 10.31 (t, *J*_{HH} = 7.5 Hz, 1H, 4' C-H), 8.63 (app t, *J*_{HH} = 7.6 Hz, 2H, 4,4" C-H), 8.00 (app t, *J*_{HH} = 6.4 Hz, 2H, 5,5" C-H), 7.52 (d, *J*_{HH} = 8.1 Hz, 2H, 3,3" C-H), 6.98 (d, *J*_{HH} = 7.6 Hz, 2H, 3',5' C-H), 1.13 (s, 2H, CH₂SiMe₃), -0.13 (s, 9H, CH₂SiMe₃) ppm. ¹³C NMR (126 MHz, benzene-*d*₆, 23 °C): δ 162.2 (2,2" CH₀), 157.2 (CH₁, 6,6" C-H), 147.7 (2',6' CH₀), 129.7 (CH₁, 4,4" C-H), 125.8 (CH₁, 5,5" C-H), 125.2 (CH₁, 3',5' C-H), 124.4 (CH₁, 3,3" C-H), 111.9 (CH₁, 4' C-H), 3.5 (CH₃, CH₂SiMe₃) ppm.

Preparation of (py)₂Co(CH₂SiMe₃)Cl. A 100 mL round bottom flask was charged with 1.37 g (2.40 mmol) of (py)₄CoCl₂ and 40 mL of pentane. A second 20 mL scintillation vial was charged with 0.282 g (2.40 mmol) of LiCH₂SiMe₃ and 5 mL of pentane. The

vials containing both mixtures were chilled in the cold well. The $\text{LiCH}_2\text{SiMe}_3$ solution was added dropwise to the warming suspension of $(\text{py})_4\text{CoCl}_2$ and a color change from pale blue to teal was observed. The resulting mixture was warmed to ambient temperature and stirred for 1 hour, during which time a color change was observed from teal to red to deep green. The volatiles were removed in vacuo and the residue was extracted with pentane (2 x 5 mL) and filtered through Celite. The filtrate was concentrated in vacuo and the resulting deep green solid was identified as $(\text{py})_2\text{Co}(\text{CH}_2\text{SiMe}_3)_2$ byproduct.³ The remaining residue was extracted with Et_2O (2 x 5 mL) and filtered through Celite. Concentration of the filtrate in vacuo and recrystallization of the dark blue residue from Et_2O /pentane at $-35\text{ }^\circ\text{C}$ for 1 hour yielded 0.782 g (77%) of analytically pure dark blue crystals of $(\text{py})_2\text{CoCl}(\text{CH}_2\text{SiMe}_3)\text{Cl}$ suitable for X-ray diffraction. Anal Calcd for $\text{C}_{14}\text{H}_{21}\text{CoN}_2\text{Si}$: C, 49.49; H, 6.23; N, 8.24. Found: C, 49.48; H, 6.19; N, 7.95. ^1H NMR (300 MHz, benzene- d_6 , $23\text{ }^\circ\text{C}$): δ 130.14 (4H br, $\Delta\nu_{1/2} = 1400\text{ Hz}$, py C-H), 40.19 (4H, $\Delta\nu_{1/2} = 168\text{ Hz}$, py C-H), 11.75 (9H, $\Delta\nu_{1/2} = 176\text{ Hz}$, CH_2SiMe_3), -2.63 (2H, $\Delta\nu_{1/2} = 67\text{ Hz}$, py C-H) ppm; 2H for CH_2SiMe_3 not observed. Magnetic Susceptibility (benzene- d_6 , $23\text{ }^\circ\text{C}$): $\mu_{\text{eff}} = 3.6\text{ }\mu_{\text{B}}$.

Preparation of $(^i\text{PrDI})\text{Co}(\text{py})\text{Cl}$. A 20 mL scintillation vial was charged with 0.126 g (0.371 mmol) of $(\text{py})_2\text{Co}(\text{CH}_2\text{SiMe}_3)\text{Cl}$ and 10 mL of pentane. While stirring, 0.150 g (0.371 mmol) $^i\text{PrDI}$ was added and the resulting solution was stirred at room temperature for 16 hours. The solution was filtered through Celite and concentrated in vacuo. The resulting residue was washed with pentane (5 x 5 mL) and the remaining green solid was collected on a glass frit and further washed with pentane to yield 0.127 g (59%) of

(ⁱPrDI)Co(py)Cl. Anal Calcd for C₃₃H₄₅ClCoN₃: C, 68.56; H, 7.85; N, 7.27. Found: C, 68.44; H, 7.52; N, 7.08. ¹H NMR (300 MHz, benzene-*d*₆, 23 °C): δ 95.01 (1H, Δ_{v1/2} = 500 Hz), 23.81 (2H, Δ_{v1/2} = 239 Hz), 11.66, (2H, Δ_{v1/2} = 325 Hz), 2.57 (12H, Δ_{v1/2} = 439 Hz), -2.55 (4H, Δ_{v1/2} = 37 Hz), -7.86 (12H, Δ_{v1/2} = 34 Hz), -21.73 (2H, Δ_{v1/2} = 16 Hz), -287.97 (6H, Δ_{v1/2} = 192 Hz) ppm; 4 resonances not located. Magnetic Susceptibility (MSB, 23 °C): μ_{eff} = 4.1 μ_B.

Preparation of (ⁱPrDI)Co(py)CH₂SiMe₃ (3). A 20 mL scintillation vial was charged with 0.175 g (0.303 mmol) of (ⁱPrDI)Co(py)Cl and 10 mL of diethyl ether and chilled to -35 °C. A 5 mL diethyl ether solution containing 0.029 g (0.303 mmol) of LiCH₂SiMe₃, chilled to -35 °C, was added dropwise and the resulting solution was warmed to ambient temperature and stirred for 30 min during which time a color change from brown to red-orange was observed. The solution was filtered through Celite and concentrated in vacuo. Recrystallization of the resulting residue from pentane at -35 °C yielded 0.134 g (70%) of (ⁱPrDI)Co(py)CH₂SiMe₃ as red crystals suitable for X-ray diffraction. Anal Calcd for C₃₇H₅₆CoN₃Si: C, 70.55; H, 8.96; N, 6.67. Found: C, 70.48; H, 8.72; N, 6.62. ¹H NMR (300 MHz, benzene-*d*₆, 23 °C): δ 79.61 (2H br, Δ_{v1/2} = 343 Hz, py C-*H*), 20.72 (2H, Δ_{v1/2} = 48 Hz, py C-*H*), 13.35 (9H, Δ_{v1/2} = 63 Hz, CH₂SiMe₃), 9.27 (1H, Δ_{v1/2} = 38 Hz, py C-*H*), 3.40 (12H, Δ_{v1/2} = 23 Hz, 4 x ⁱPr CH₃), -3.10 (4H, Δ_{v1/2} = 17 Hz), -5.41 (12H, Δ_{v1/2} = 33 Hz, 4 x ⁱPr CH₃), -19.47 (2H, Δ_{v1/2} = 20 Hz), -252.41 (6H, Δ_{v1/2} = 195 Hz, 2 x imine CH₃) ppm; 6 x H residues not found. Magnetic Susceptibility (MSB, 23 °C): μ_{eff} = 3.3 μ_B.

Preparation of [(ⁱPrDI)CoCl]₂. A 20 mL scintillation vial was charged with 0.368 g (0.689 mmol) of (ⁱPrDI)CoCl₂¹⁷ and 10 mL of diethyl ether and chilled to -35 °C. A 5 mL diethyl ether solution containing 0.065 g (0.689 mmol) of LiCH₂SiMe₃, chilled to -35 °C, was added dropwise and the resulting solution was allowed to warm to room temperature and stir for 1 during which time a color change from brown to green was observed. The solution was filtered through Celite and concentrated in vacuo. The residue was washed with pentane and the remaining green solid was collected on a glass frit to yield 0.250 g (73%) of [(ⁱPrDI)CoCl]₂. Spectroscopic data are consistent with those reported previously.¹⁷

Preparation of (ⁱPrDI)Co(η³-C₃H₅) (4). A 20 mL scintillation vial was charged with 0.114 g (0.114 mmol) of [(ⁱPrDI)CoCl]₂ and 10 mL of diethyl ether and chilled to -35 °C. While stirring, 0.134 mL of allyl magnesium chloride solution (1.7 M in THF, 0.228 mmol) was added dropwise via microsyringe. The resulting solution was warmed to ambient temperature and stirred for 10 minutes during which time a color change from green to teal was observed. The solution was filtered through celite and concentrated in vacuo. Recrystallization of the resulting residue from pentane at -35 °C yielded 0.084 g (73%) of (ⁱPrDI)Co(η³-C₃H₅) as green crystals suitable for X-ray diffraction. Anal Calcd for C₃₁H₄₅CoN₂: C, 73.78; H, 8.99; N, 5.55. Found: C, 73.48; H, 8.64; N, 5.34. ¹H NMR (500 MHz, toluene-*d*₈, 21.7 °C): δ 11.19 (tt, *J*_{HH} = 12.5, 5.9 Hz, 1H, *meso* allyl C-H), 10.28 (d, *J*_{HH} = 5.9 Hz, 2H, *syn* allyl C-H), 7.55 (t, *J*_{HH} = 7.9 Hz, 2H, *p*-Ar C-H), 7.09 (obsc d, *J*_{HH} = 7.9 Hz, 4H, *m*-Ar C-H), 2.02 (obsc br m, 4H, CH(CH₃)₂), 1.06 (d, *J*_{HH} = 6.8 Hz, 12H, two of CH(CH₃)₂), 0.57 (d, *J*_{HH} = 6.8 Hz, 12H, two of CH(CH₃)₂), -0.21 (d, *J*_{HH} = 12.5 Hz, 2H,

anti allyl C-H), -5.60 (s, 6H, imine CH₃) ppm. ¹H NMR (500 MHz, benzene-*d*₆, 23 °C): δ 11.26, 10.47, 7.61, 7.16, 2.06, 1.06, 0.59, -0.13, -5.63 ppm. ¹³C NMR (126 MHz, benzene-*d*₆, 23 °C): δ 166.8 (CH₀, imine C=N-C), 166.2 (CH₀, imine C=N-C), 133.7 (CH₁, allyl C-H), 128.7 (CH₀, imine *o*-Ar), 125.1 (CH₁, imine *p*-Ar), 122.7 (CH₁, imine *m*-Ar), 34.5 (CH₂, allyl CH₂), 31.3 (CH₃, imine CH₃C=N), 28.8 (CH₁, CH(CH₃)₂), 23.5 (CH₃, one of CH(CH₃)₂), 23.2 (CH₃, one of CH(CH₃)₂) ppm.

Preparation of (ⁱPrDI)Co(py-*d*₅)CH₂SiMe₃ (3-*d*₅). A 20 mL scintillation vial was charged with 0.051 g (0.051 mmol) of [(ⁱPrDI)CoCl]₂ and 5 mL of diethyl ether and chilled to -35 °C. While stirring, a 5 mL diethyl ether solution containing 0.010 g (0.106 mmol) of LiCH₂SiMe₃, chilled to -35 °C, was added dropwise. The resulting solution was warmed to ambient temperature and stirred for 5 min during which time a color change from green to red-orange was observed. At the observation of the color change, 0.013 mL (0.159 mmol) of pyridine-*d*₅ was added and a color change from red-orange to red was observed. The solution was filtered through celite and concentrated and the remaining residue was dissolved in pentane, transferred to a pre-weighed 20 mL scintillation vial, and concentrated to yield 0.063 g (93%) (ⁱPrDI)Co(py-*d*₅)CH₂SiMe₃ as a red solid. ¹H NMR (300 MHz, benzene-*d*₆, 23 °C): δ 13.50 (9H, Δ_{v1/2} = 82 Hz, CH₂SiMe₃), 3.40 (12H, Δ_{v1/2} = 45 Hz, 4 x *i*Pr CH₃), -3.12 (4H, Δ_{v1/2} = 34 Hz), -5.42 (12H, Δ_{v1/2} = 50 Hz, 4 x *i*Pr CH₃), -19.46 (2H, Δ_{v1/2} = 34 Hz), -252.44 (6H, Δ_{v1/2} = 205 Hz, 2 x imine CH₃) ppm; 6 x H residues not found. The spectrum is consistent with that of **3** with pyridine C-H residues removed by isotopic substitution.

Preparation of (ⁱPrDI)Co(η^3 -limonene) (5). A 20 mL scintillation vial was charged with 0.030 g (0.059 mmol) of (ⁱPrDI)Co(η^3 -C₃H₅) and 8 mL of diethyl ether. While stirring, 0.016 g of pinacolborane (0.125 mmol) was added. After 5 minutes, 0.017 g of limonene (0.125 mmol) was added. The resulting solution was stirred for 30 minutes during which time a color change from teal to green to orange was observed. The solution was concentrated in vacuo. Recrystallization of the resulting residue from pentane at -35 °C yielded 0.015 g (41%) of **5** as orange crystals suitable for X-ray diffraction. ¹H NMR (300 MHz, benzene-*d*₆, 23 °C): δ 7.45 (t, J_{HH} = 7.8 Hz, 2H, *p*-Ar C-H), 7.29 (t, J_{HH} = 7.8 Hz, 2H, *p*-Ar C-H), 5.00 (d, J_{HH} = 3.2 Hz, 2H, agostic CH), 4.19 (br, 2H, two of iPr CH), 2.99 (br, 2H, two of iPr CH), 2.30 (s, 3H, *meso* allyl CH₃), 1.51 (br, 12H, four of CH₃), 1.13 (br, 6H, two of iPr CH₃), 0.92 (br, 6H, two of iPr CH₃), 0.48 (m, 1H, limonene iPr CH), 0.41 (d, J_{HH} = 5.3 Hz, 6H, two of limonene iPr CH₃), 0.36 (br, 2H, CH), -0.74 (br, 1H, ring CH), -1.07 (s, 6H, imine CH₃), -6.42 (dd, J_{HH} = 15.5, 10.2 Hz, 2H, allyl CH) ppm. ¹³C NMR (126 MHz, benzene-*d*₆, 23 °C): δ 157.5 (CH₀, imine C=N-C), 148.1 (CH₀, imine C=N-C), 136.3 (CH₀, allyl CH₀), 125.4 (CH₁, imine *p*-Ar), 123.5 (CH₁, imine *m*-Ar), 123.0 (CH₁, imine *m*-Ar), 111.7 (CH₀, imine *o*-Ar), 56.7 (CH₂, agostic CH), 36.1 (CH₁, limonene ring CH), 32.3 (CH₁, limonene iPr CH), 24.8 (CH₃, Ar iPr CH₃) 23.5 (CH₃, imine CH₃C=N), 20.6 (CH₃, limonene iPr CH₃), 19.5 (CH₃, limonene Me CH₃) ppm.

III. Procedures for Catalytic Olefin Hydroboration and Pyridine Exchange.

A. General Procedure for Catalytic Olefin Hydroboration. In a typical experiment, a scintillation vial (with a magnetic stir bar) was charged in the glovebox with 0.64 mL tert-butyl methyl ether, 0.64 mmol (1 eq) of the desired olefin, 0.67 mmol (1.05 eq) of

pinacolborane, 0.64 mmol (1 eq) cyclooctane internal standard, and 1 mol% of the cobalt pre-catalyst. The vial was capped and the mixture was stirred at 23 °C until the reaction was complete. The reaction was monitored by analysis of aliquots by gas chromatography. Upon completion, the mixture was concentrated, diluted with hexane and passed through a silica plug in a Pasteur pipette and concentrated *in vacuo*. The resulting solution was concentrated and then analyzed by GC-FID, ¹H NMR, and ¹³C NMR to determine the purity, identity, and regioisomeric and diastereomeric ratio of products. Partial conversions were determined by comparing the ratio of substrate to internal standard to the ratio obtained in an initial aliquot taken at the beginning of the reaction.

B. Procedure for Pyridine Exchange Experiment. In a J. Young NMR tube, a benzene-*d*₆ solution containing .011 g (0.017 mmol) **3-*d*₅** was prepared and analyzed by ¹H NMR. Approximately 3 μL (.003 g, 0.037 mmol) pyridine was then added via microsyringe. The solution was analyzed by ¹H NMR after 90 minutes, during which time three signals with chemical shifts at 9.27, 20.72 and 79.61 ppm began to grow in corresponding to coordinated pyridine in **3**. Free pyridine signals were also still visible.

C. Procedure for Pyridine Inhibition Studies. In a typical experiment, a scintillation vial (with a magnetic stir bar) was charged in the glovebox with 1 mol% **4**, 0.64 mL tert-butyl methyl ether, 0.64 mmol (1 eq) of 1-octene, 0.64 mmol (1 eq) cyclooctane as an internal standard, and the desired mol% of pyridine additive. Via microsyringe, 0.67 mmol (1.05 eq) of pinacolborane was then added, the vial was capped and the mixture

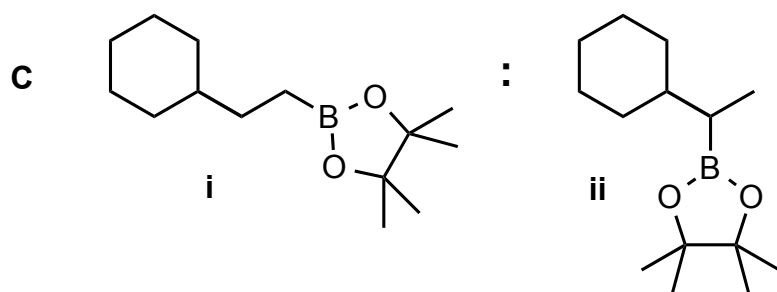
D. Procedure for Limonene Inhibition Study. A 20 mL scintillation vial (with magnetic stir bar) was charged in the glovebox with 0.64 mL tert-butyl methyl ether, 0.031 g (0.32 mmol) of 2,3,3-trimethyl-1-butene, 0.044 g (0.32 mmol) of limonene, 0.003 g (0.006 mmol) of **4**, and 0.036 g (0.32 mmol) cyclooctane internal standard. An initial aliquot was taken for reference, then 0.086 g (0.67 mmol) of pinacolborane was added. The vial was capped and the mixture was stirred at 23 °C and monitored by gas chromatography to determine substrate conversions. After 18 hours, an gas chromatographic analysis showed <5% conversion of 2,3,3-trimethyl-1-butene starting material and 50% conversion of limonene starting material, determined by internal standard referenced with the initial aliquot.

A

i

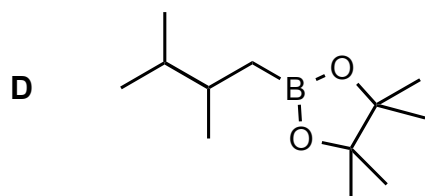
ii

Chemical structures of two boronate esters, labeled i and ii, separated by a colon. Structure i is a linear boronate ester with a heptyl chain and a 2,2,4,4-tetramethyl-1,3-dioxolane-5-yl group. Structure ii is a cyclic boronate ester with a 2,2,4,4-tetramethyl-1,3-dioxolane-5-yl group and a 2,2,4,4-tetramethyl-1,3-dioxolane-5-yl group.



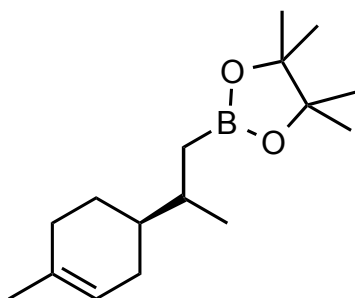
2-(2-cyclohexylethyl)-4,4,5,5-tetramethyl-1,3,2-dioxaborolane (C-i). ^1H NMR (500 MHz, chloroform-*d*, 23 °C): δ 1.74-1.59 (m, 5H), 1.32-1.26 (m, 2H), 1.24 (s, 12H), 1.21-1.07 (m, 4H), 0.88-0.78 (m, 2H), 0.75 (t, 7.1 Hz, 2H) ppm. ^{13}C NMR (126 MHz, chloroform-*d*, 23 °C): δ 83.0, 40.1, 33.1, 31.5, 26.9, 26.6, 25.0 ppm. ^1H and ^{13}C NMR data agree with previously reported data.²

2-(1-cyclohexylethyl)-4,4,5,5-tetramethyl-1,3,2-dioxaborolane (C-ii). The ^1H NMR spectrum was not assigned since the proton resonances are obscured by those of the major regioisomer **a**. ^{13}C NMR (126 MHz, chloroform-*d*, 23 °C): δ 82.7, 40.5, 32.7, 31.9, 27.0, 26.8, 24.9, 24.8, 12.6 ppm. The ^{13}C NMR data agree with previously reported data.¹⁸



2-(2,3-dimethylbutyl)-4,4,5,5-tetramethyl-1,3,2-dioxaborolane (D). ^1H NMR (500 MHz, chloroform-*d*, 23 °C): δ 1.59 (app dddt, J_{HH} = 11.7, 6.8, 4.9, 1.9 Hz, 1H), 1.47 (pd, J_{HH} = 6.8, 4.9 Hz, 1H), 0.86-0.79 (overlapping doublets, 10H), 0.60 (dd, J_{HH} = 15.2, 9.9 Hz, 1H) ppm. ^{13}C NMR (126 MHz, chloroform-*d*, 23 °C): δ 83.0, 35.2, 34.3, 25.1, 24.9, 19.9, 18.8, 18.7 ppm. ^1H and ^{13}C NMR data agree with previously reported data.²

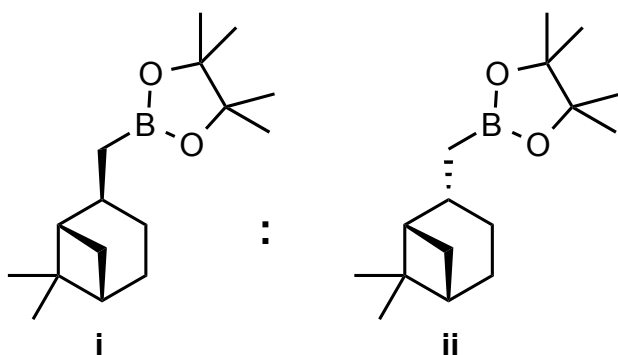
E



(+/-)-2-(2-(4-methylcyclohex-3-en-1-yl)propyl)-4,4,5,5-tetramethyl-1,3,2-

dioxaborolane (E). Diastereomers of this compound were not distinguished by ^1H or ^{13}C NMR due to overlapping resonances. ^1H NMR (500 MHz, chloroform-*d*, 23 °C): δ 5.36 (br s, 1H), 2.02-1.86 (m, 3H), 1.77-1.64 (m, 3H), 1.62 (s, 3H), 1.33-1.15 (m, 2H), 1.25 (s, 6H), 1.24 (s, 6H), 0.92-0.86 (m, 4H), 0.61 (dd, $J_{HH} = 15.3, 9.9$ Hz, 1H) ppm. ^{13}C NMR (126 MHz, chloroform-*d*, 23 °C): δ 134.0, 121.2, 83.0, 40.8, 34.0, 33.9, 31.1, 29.3, 28.5, 26.9, 26.0, 25.1, 24.9, 23.6, 19.5, 19.2 ppm. ^1H and ^{13}C NMR data agree with previously reported data.¹⁹

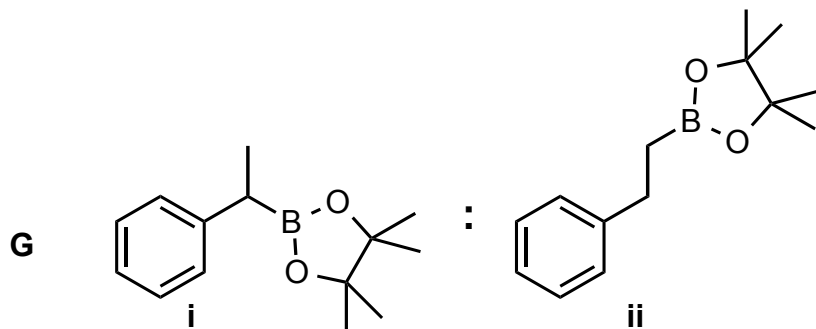
F



2-(((2R)-6,6-dimethylbicyclo[3.1.1]heptan-2-yl)methyl)-4,4,5,5-tetramethyl-1,3,2-

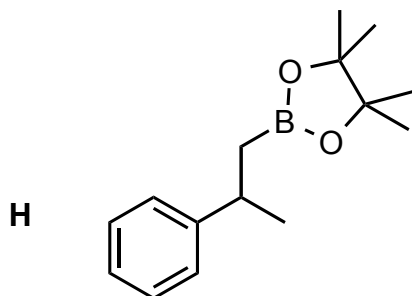
dioxaborolane (F-i). The ^1H NMR spectrum was not assigned because overlapping proton resonances from both diastereomers. ^{13}C NMR (126 MHz, chloroform-*d*, 23 °C): δ 82.9, 48.7, 40.8, 39.7, 38.9, 31.3, 27.0, 26.8, 24.9, 24.4, 23.2, 20.3 ppm. ^1H and ^{13}C NMR data agree with previously reported data.²

2-(((2S)-6,6-dimethylbicyclo[3.1.1]heptan-2-yl)methyl)-4,4,5,5-tetramethyl-1,3,2-dioxaborolane (F-ii). The ^1H NMR spectrum was not assigned because overlapping proton resonances from both diastereomers. ^{13}C NMR (126 MHz, chloroform-*d*, 23 °C): δ 82.9, 48.9, 41.4, 38.9, 37.4, 34.1, 28.4, 26.7, 25.0, 24.8, 24.4, 23.3 ppm. ^1H and ^{13}C NMR data agree with previously reported data.²

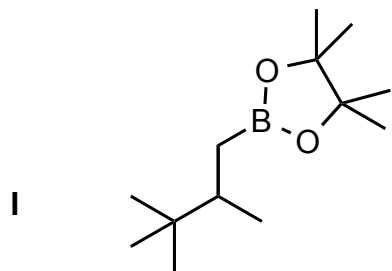


2-(1-phenethyl)-4,4,5,5-tetramethyl-1,3,2-dioxaborolane (G-i). ^1H NMR (500 MHz, chloroform-*d*, 23 °C): δ 7.29-7.20 (m, 4H), 7.16-7.11 (m, 1H), 2.44 (q, $J_{\text{HH}} = 7.4$ Hz, 1H), 1.33 (d, $J_{\text{HH}} = 7.4$ Hz, 3H), 1.22 (s, 6H), 1.20 (s, 6H) ppm. ^{13}C NMR (126 MHz, chloroform-*d*, 23 °C): δ 145.1, 128.4, 127.9, 125.2, 83.4, 24.8, 24.7, 17.2 ppm. ^1H and ^{13}C NMR data agree with previously reported data.²⁰

2-(2-phenethyl)-4,4,5,5-tetramethyl-1,3,2-dioxaborolane (G-ii). ^1H NMR (500 MHz, chloroform-*d*, 23 °C): δ 2.75 (t, $J_{\text{HH}} = 8.1$ Hz), 1.24 (s, 12H) ppm. The remaining proton resonances were not assigned since they are obscured by those of the major regioisomer **a**. ^{13}C NMR (126 MHz, chloroform-*d*, 23 °C): δ 144.5, 128.3, 128.1, 125.6, 83.2, 30.1, 24.9 ppm. ^1H and ^{13}C NMR data agree with previously reported data.¹⁹

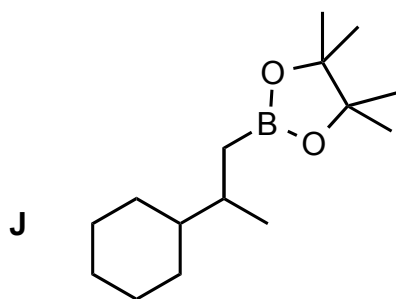


2-(2-phenylpropyl)-4,4,5,5-tetramethyl-1,3,2-dioxaborolane (H). ^1H NMR (500 MHz, chloroform-*d*, 23 °C): δ 7.29-7.24 (m, 4H), 7.18-7.13 (m, 1H), 3.03 (app h, $J_{\text{HH}} = 7.1$ Hz, 1H), 1.28 (d, $J_{\text{HH}} = 7.0$ Hz, 3H), 1.20 (m, 2H), 1.16 (s, 12H) ppm. ^{13}C NMR (126 MHz, chloroform-*d*, 23 °C): δ 149.3, 128.3, 126.7, 125.8, 83.1, 35.9, 25.0, 24.9, 24.8 ppm. ^1H and ^{13}C NMR data agree with previously reported data.²

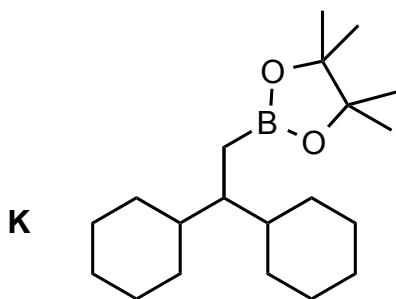


2-(2,3,3-trimethylbutyl)-4,4,5,5-tetramethyl-1,3,2-dioxaborolane (I). The title compound was isolated as a colorless oil. ^1H NMR (500 MHz, chloroform-*d*, 23 °C) δ 1.53 (app ddt, $J_{\text{HH}} = 10.8, 6.9, 3.5$ Hz, 1H, tBuCHCH₃), 1.26 (s, 6H, two of pinacol CH₃), 1.25 (s, 6H, two of pinacol CH₃), 0.95 (dd, $J_{\text{HH}} = 15.4, 3.7$ Hz, 1H, one of CH₂BPin), 0.86 (d, $J_{\text{HH}} = 6.4$ Hz, 3H, tBuCHCH₃), 0.83 (s, 9H, tBu methyls), 0.50 (dd, $J_{\text{HH}} = 15.2, 11.1$ Hz, 1H, one of CH₂BPin). ^{13}C NMR (126 MHz, chloroform-*d*, 23 °C): δ 83.0 (CH₀, pinacol C(CH₃)₂), 39.2 (CH₃), 33.5 (CH₀, tBu C(CH₃)₃), 27.2 (CH₃), 25.1 (CH₃), 24.8 (CH₃), 17.5 (CH₃) ppm. GCMS *m/z* (% relative intensity, ion) 226.2 (0.03%, M⁺), 211.2

(6%, M^+ -15), 171.1 (12%, M^+ -55), 126.2 (6%, M^+ -100), 101.1 (17%, M^+ -125), 83.1 (18%, M^+ -143), 69.1 (14%, M^+ -157), 57.1 (26%, M^+ -169).

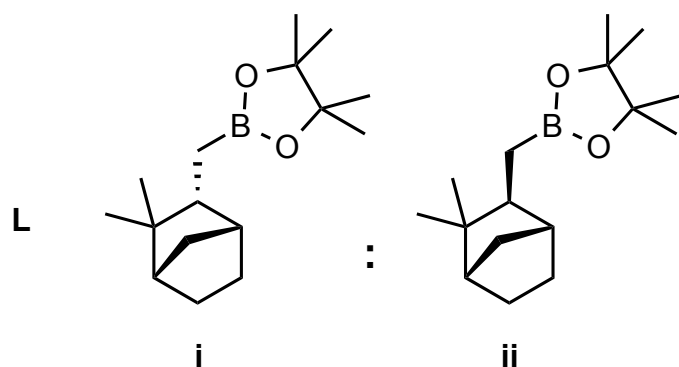


2-(2-cyclohexylpropyl)-4,4,5,5-tetramethyl-1,3,2-dioxaborolane (J) ^1H NMR (500 MHz, chloroform-*d*, 23 °C): δ 1.75-1.53 (m, 6H), 1.25 (s, 6H), 1.24 (s, 6H), 1.18-1.03 (m, 4H), 1.00-0.86 (m, 2H), 0.86 (d, J_{HH} = 6.8 Hz, 3H), 0.82 (d, J_{HH} = 4.6 Hz, 1H), 0.59 (dd, J_{HH} = 9.8, 15.2 Hz, 1H) ppm. ^{13}C NMR (126 MHz, chloroform-*d*, 23 °C): δ 82.9, 45.0, 34.7, 30.5, 29.3, 27.1, 27.0, 26.9, 25.1, 24.9, 19.3 ppm. ^1H and ^{13}C NMR data agree with previously reported data.²¹



2-(2,2-dicyclohexylethyl)-4,4,5,5-tetramethyl-1,3,2-dioxaborolane (K) The title compound was isolated as a colorless oil. ^1H NMR (500 MHz, chloroform-*d*, 23 °C): δ 1.73-1.55 (m, 10H), 1.33-1.26 (m, 3H), 1.23 (s, 12H, 4 x pinacol CH_3), 1.20-0.89 (m, 10H), 0.63 (d, J_{HH} = 5.6 Hz, CH_2BPin) ppm. ^{13}C NMR (126 MHz, chloroform-*d*, 23 °C): δ 82.9, 45.1, 40.6, 32.0, 29.5, 27.2, 27.0, 24.9 ppm. GCMS m/z (% relative intensity,

ion) 320.3 (0.28%, M^+), 305.3 (2%, M^+-15), 237.2 (14%, M^+-83), 179.1 (3%, M^+-141), 137.1 (6%, M^+-183), 109.1 (24%, M^+-211), 83.1 (20%, M^+-237), 55.1 (30%, M^+-265).



2-(((2R)-3,3-dimethylbicyclo[2.2.1]heptan-2-yl-methyl)-4,4,5,5-tetramethyl-1,3,2-dioxaborolane (L-i). The mixture of diastereomers was isolated as a white solid. The ^1H NMR spectrum was not assigned because overlapping proton resonances from both diastereomers. ^{13}C NMR (126 MHz, chloroform-*d*, 23 °C): δ 82.9, 49.2, 46.1, 37.1, 32.1, 29.8, 25.0, 24.9, 24.8, 24.7, 22.0, 20.1 ppm. GCMS m/z (% relative intensity, ion) 251.9 (0.24%, M^+-12), 136.1 (4%, M^+-128), 121.1 (9%, M^+-143), 111.1 (7%, M^+-153), 93.1 (22%, M^+-171), 79.1 (10%, M^+-185), 67.1 (20%, M^+-197), 55.1 (8%, M^+-209), 41.1 (19%, M^+-223).

2-(((2S)-3,3-dimethylbicyclo[2.2.1]heptan-2-yl-methyl)-4,4,5,5-tetramethyl-1,3,2-dioxaborolane (L-ii). The ^1H NMR spectrum was not assigned because of overlap of the resonances between diastereomers. ^{13}C NMR (126 MHz, chloroform-*d*, 23 °C): δ 82.9, 49.8, 49.4, 46.5, 40.7, 37.2, 35.5, 27.8, 25.0, 24.9, 25.6, 24.3 ppm

V. Additional Structural and NMR Spectroscopic Data

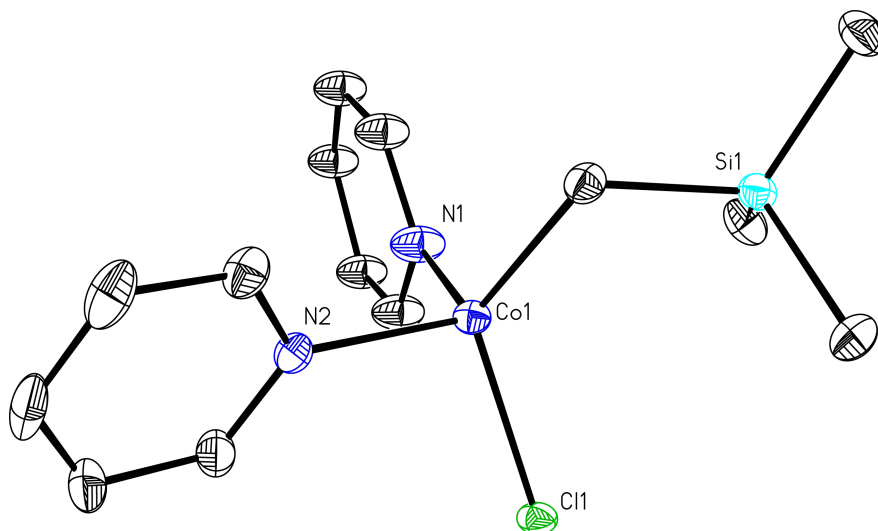


Figure S1. Solid state molecular structure of $(\text{Py})_2\text{Co}(\text{CH}_2\text{SiMe}_3)\text{Cl}$ at 30% probability ellipsoids. Hydrogen atoms were omitted for clarity.

Table S1. Selected bond distances in $(\text{py})_2\text{Co}(\text{CH}_2\text{SiMe}_3)\text{Cl}$

Bond	Distance, Å	Bond	Distance, Å
N1-Co1	2.060(2)	Cl1-Co1	2.3052(6)
N2-Co1	2.0581(19)	C11-Co1	2.006(2)

Table S2. Selected bond angles in $(\text{py})_2\text{Co}(\text{CH}_2\text{SiMe}_3)\text{Cl}$.

Atoms	Bond Angle, °
N1-Co1-N2	103.65(9)
N1-Co1-Cl1	102.07(6)
N1-Co1-C11	110.60(9)
N2-Co1-Cl1	103.42(5)
N2-Co1-C11	110.21(8)
Cl1-Co1-C11	124.74(7)

Table S3. Selected bond distances in **2**.

Bond	Distance, Å	Bond	Distance, Å
N1-C5	1.373(7)	C10-C11	1.447(7)
N2-C6	1.366(7)	N1-Co1	1.919(4)
N2-C10	1.362(7)	N2-Co1	1.832(4)
N3-C11	1.380(7)	N3-Co1	1.911(4)
C5-C6	1.447(8)	C16-Co1	1.972(5)

Table S4. Selected bond angles in **2**.

Atoms	Bond Angle, °
N1-Co1-N2	81.55(19)
N1-Co1-C16	98.5(2)
N2-Co1-N3	81.86(18)
N3-Co1-C16	98.1(2)
N2-Co1-C16	98.5(2)

Table S5. Selected bond distances in **3**.

Bond	Distance, Å	Bond	Distance, Å
N1-C2	1.3396(18)	N2-Co1	1.9705(12)
N2-C3	1.3468(18)	N3-Co1	2.0131(15)
C2-C3	1.417(2)	C29-Co1	2.0432(12)
N1-Co1	1.9575(11)		

Table S6. Selected bond angles in **3**.

Atoms	Bond Angle, °
N1-Co1-N2	81.33(5)
N1-Co1-C29	114.90(5)
N2-Co1-C29	132.16(6)
N1-Co1-N3	114.04(5)
N2-Co1-N3	112.74(5)
N3-Co1-C29	101.22(5)

Table S7. Selected bond distances in **4**.

Bond	Distance, Å	Bond	Distance, Å
N1-C2	1.329(3)	C15-Co1	2.016(3)
C2-C2A	1.427(4)	C16-Co1	1.951(5)
N1-Co1	1.8988(11)	C15A-Co1	2.016(3)
N1A-Co1	1.8988(11)		

Table S8. Selected bond angles in **4**.

Atoms	Bond Angle, °
N1-Co1-N1A	81.50(11)
N1-Co1-C15	174.86(10)
N1-Co1-C15A	102.49(10)
N1-Co1-C16	140.53(16)
C15-C16-C15A	126.5(4)

Table S9. Selected bond distances in **5**.

Bond	Distance, Å	Bond	Distance, Å
N1-C2	1.3440(17)	C29-Co1	2.0177(14)
N2-C3	1.3312(17)	C30-Co1	2.0260(14)
C2-C3	1.4111(19)	C34-Co1	1.9920(16)
N1-Co1	1.8736(14)	H33A-C33	1.0052(90)
N2-Co1	1.9184(12)	H33A-Co1	1.8861(44)
		C33-Co1	2.3041(15)

Table S10. Selected bond angles in **5**.

Atoms	Bond Angle, °
N1-Co1-N2	81.94(5)
N1-Co1-C29	128.03(5)
N2-Co1-C29	130.25(5)
N1-Co1-C30	101.29(5)
N2-Co1-C30	170.57(5)
N1-Co1-C34	168.34(5)
N2-Co1-C34	103.41(5)
C30-C29-C34	102.7(10)
Co1-H33A-C33	101.3

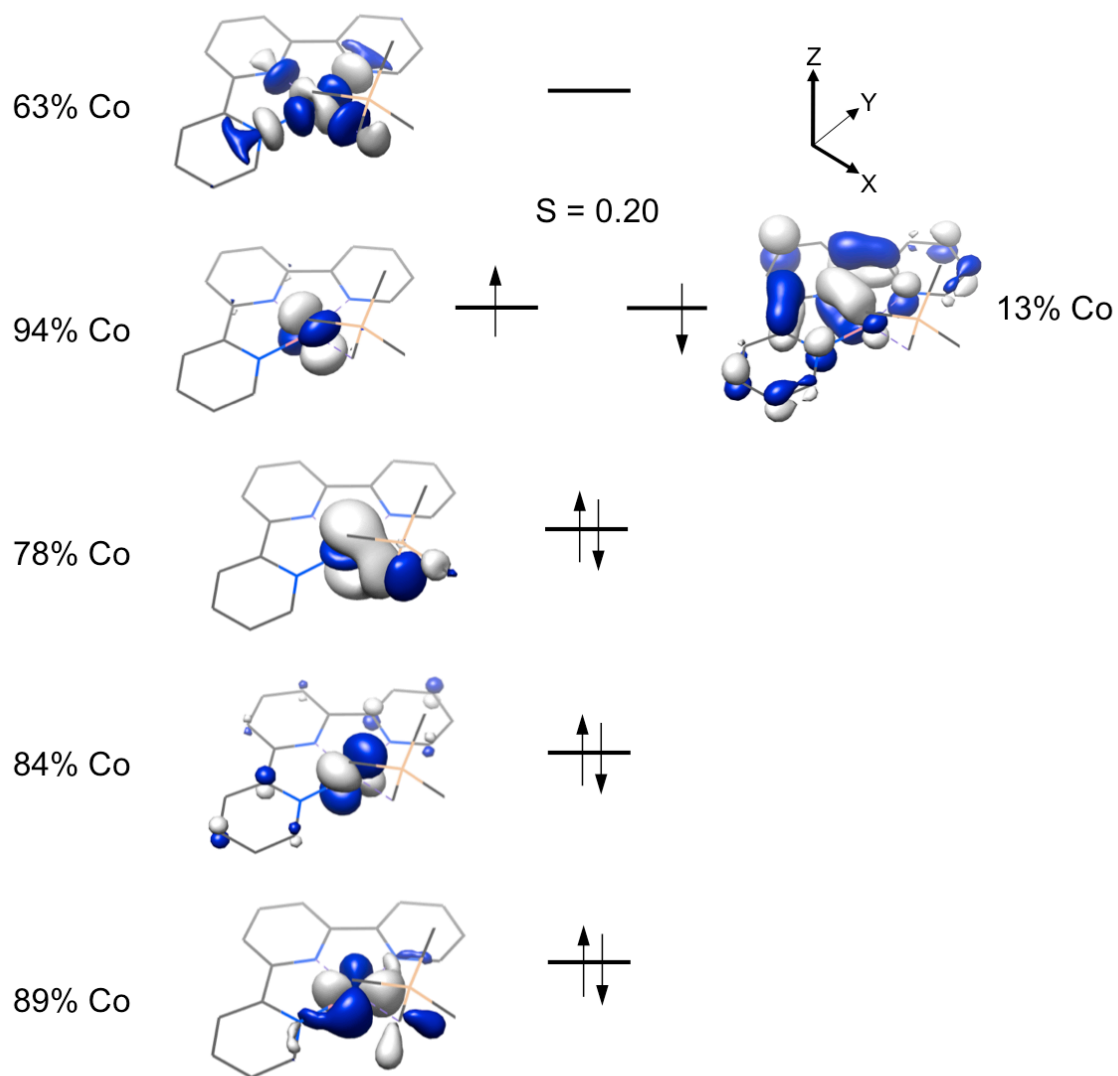


Figure S2. Qualitative molecular orbital diagram for **2** from a geometry-optimized B3LYP DFT calculation.

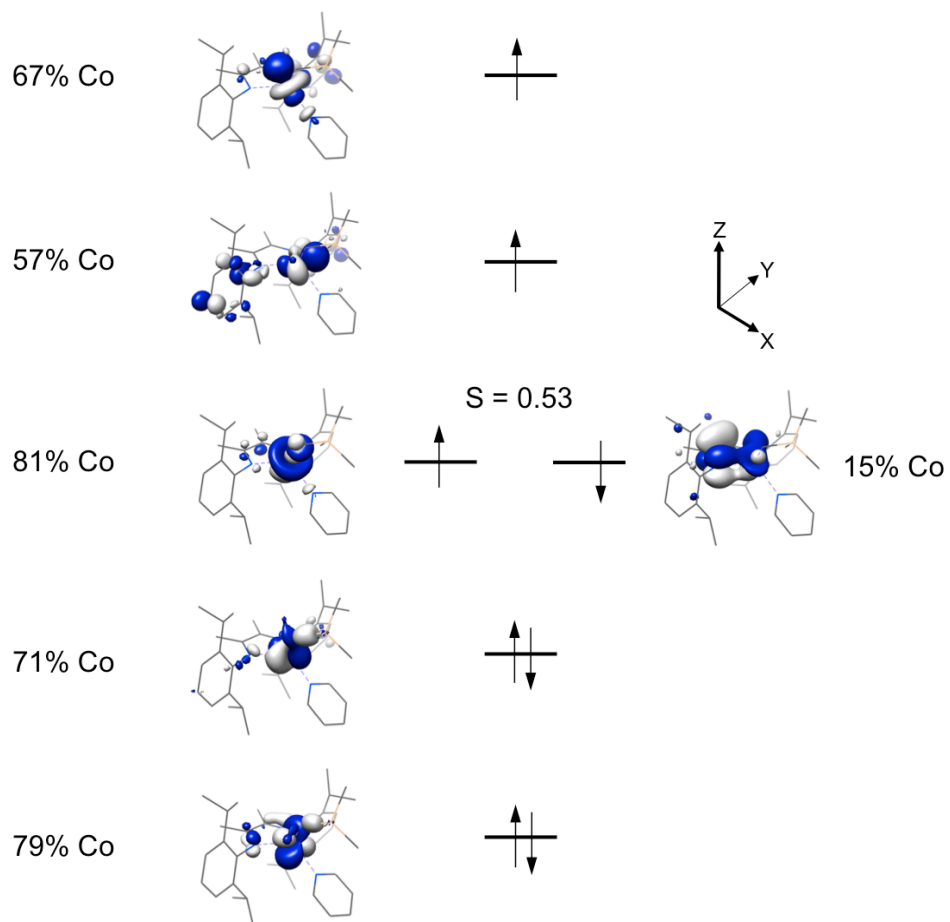


Figure S3. Qualitative molecular orbital diagram for **3** from a geometry-optimized B3LYP DFT calculation.

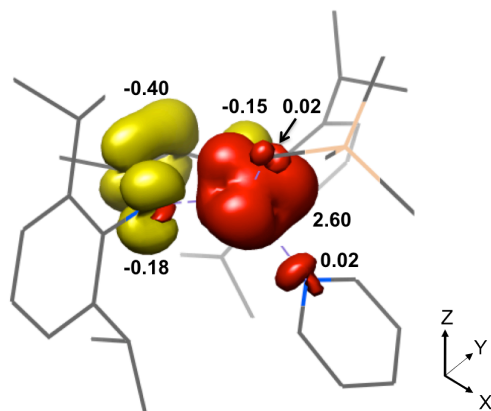


Figure S4. Mulliken spin density plot for **3** from a geometry-optimized B3LYP DFT calculation.

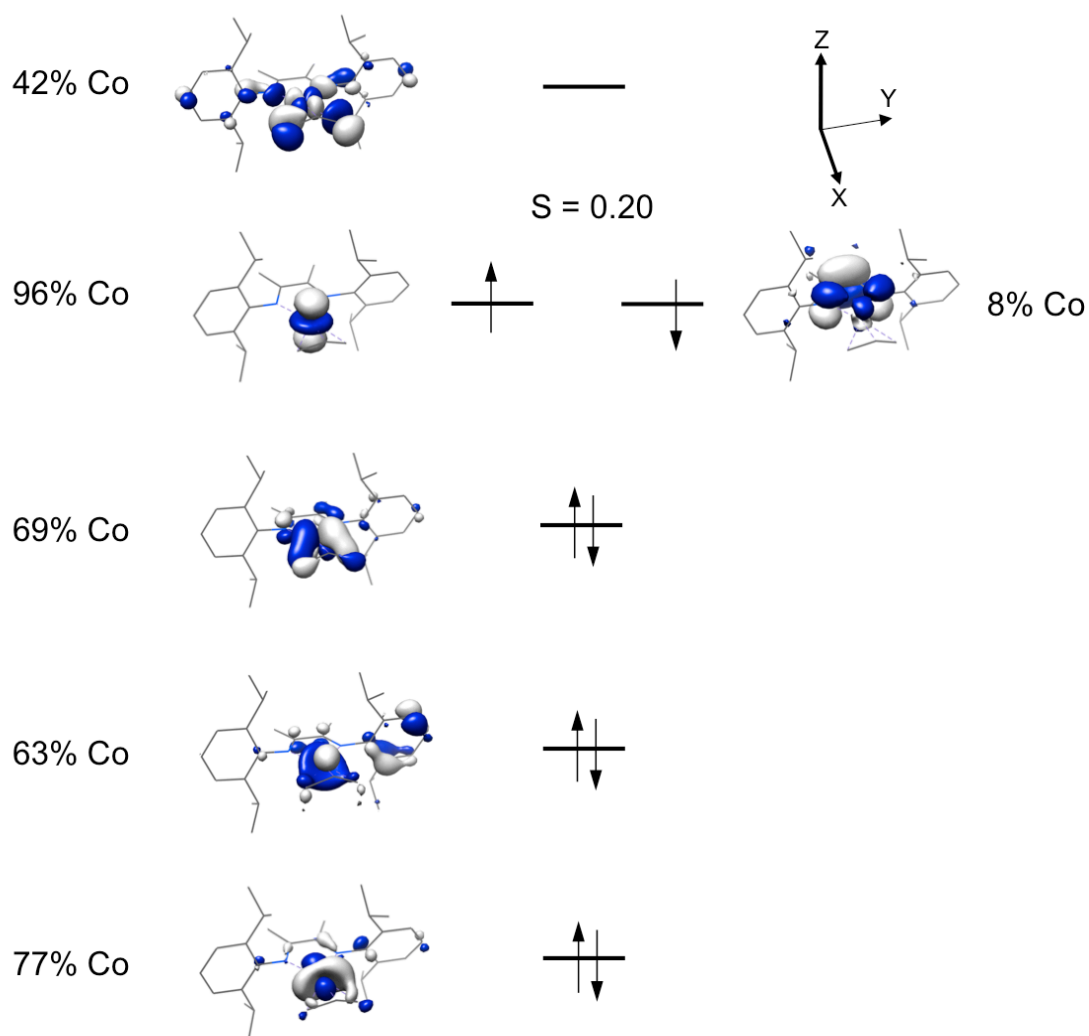


Figure S5. Qualitative molecular orbital diagram for **4** from a geometry-optimized B3LYP DFT calculation.

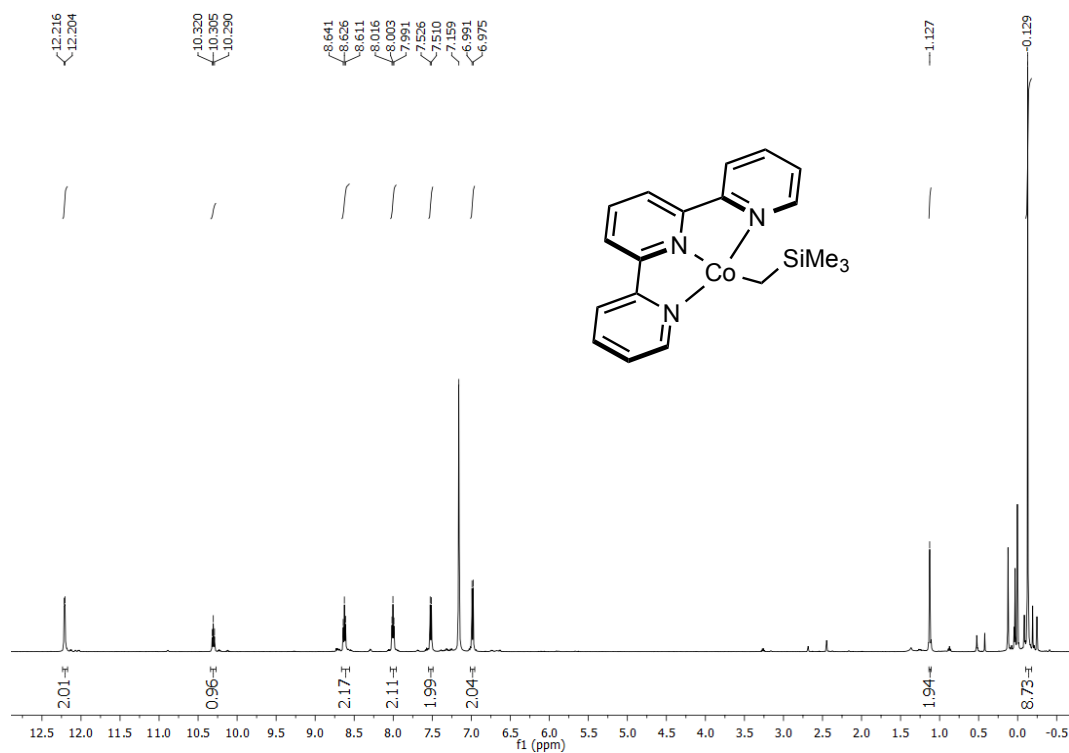


Figure S6. ^1H NMR spectrum (500 MHz, C_6D_6 , 23 $^\circ\text{C}$) of **2**. Tetramethylsilane and other trace organic impurities were also observed in the region between -0.5 and 5 ppm.

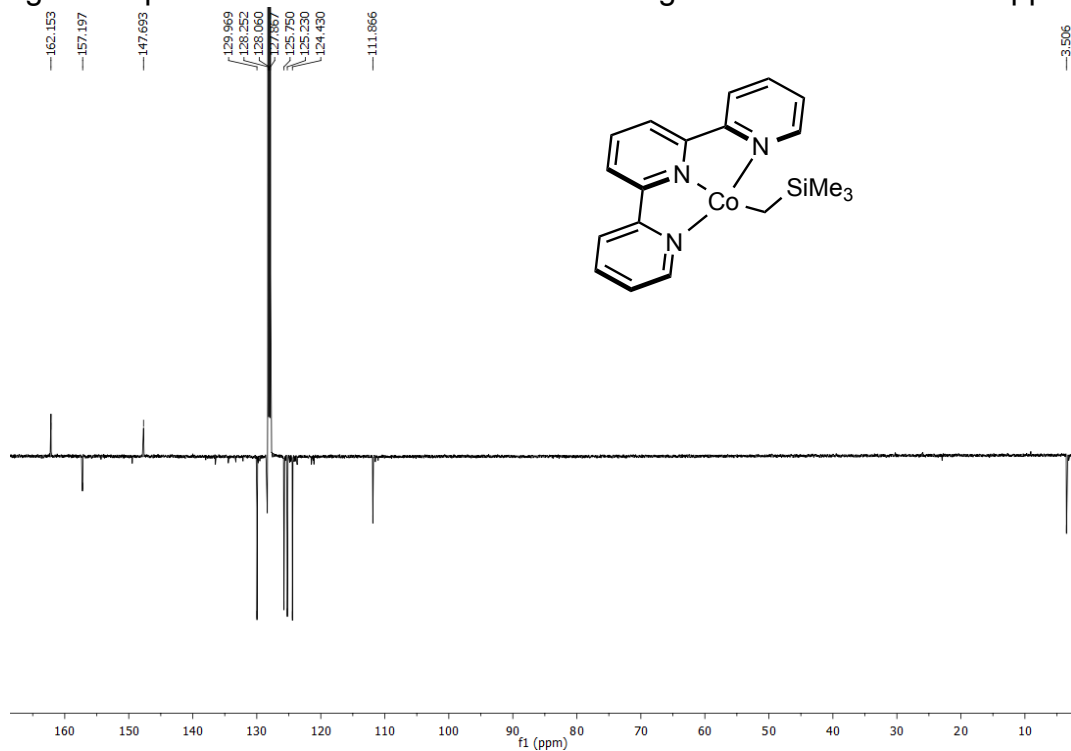


Figure S7. ^{13}C attached proton test NMR spectrum (126 MHz, C_6D_6 , 23 $^\circ\text{C}$) of **2**.

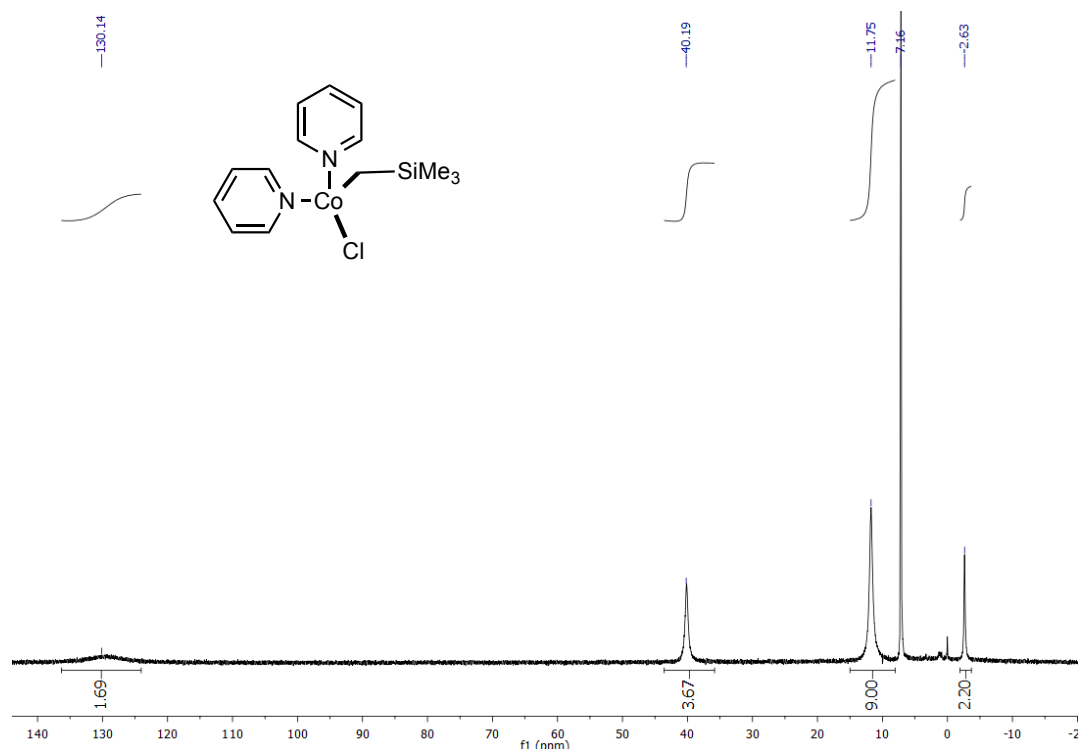


Figure S8. ^1H NMR spectrum (300 MHz, C_6D_6 , 23 °C) of $(\text{py})_2\text{Co}(\text{CH}_2\text{SiMe}_3)\text{Cl}$.

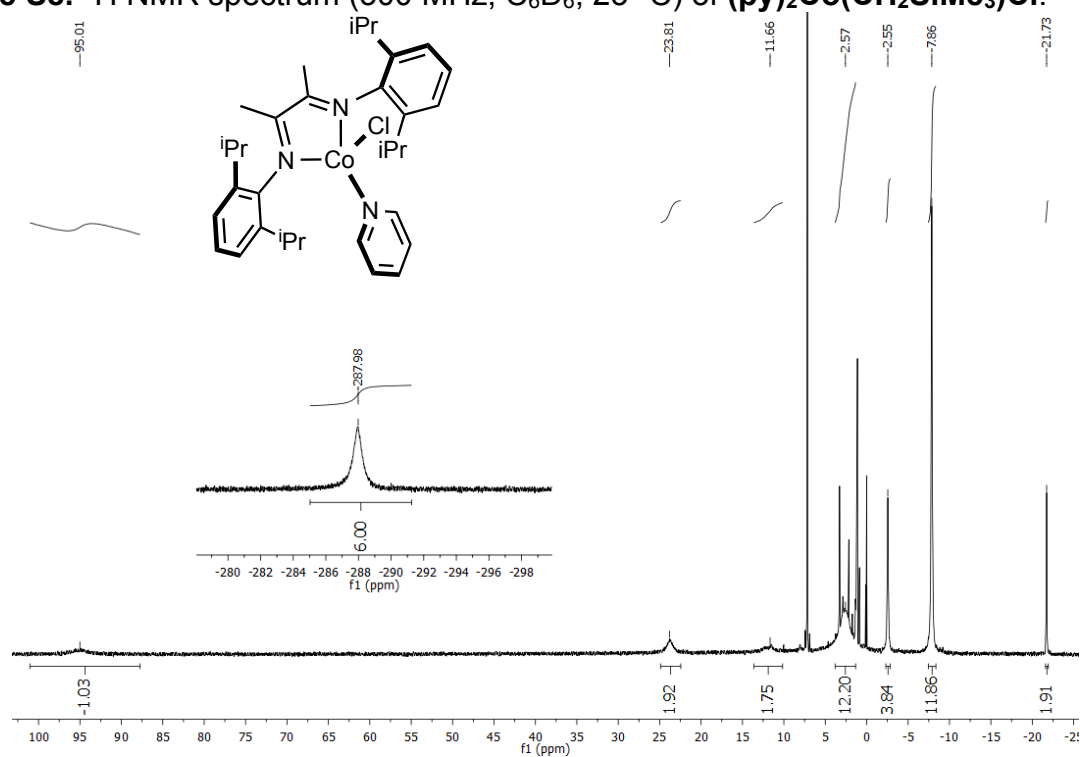


Figure S9. ^1H NMR spectrum (300 MHz, C_6D_6 , 23 °C) of $(\text{iPrDI})\text{Co}(\text{py})\text{Cl}$. Diethyl ether, tetramethylsilane, and other residual organic solvents were also observed in the region between 0 and 5 ppm.

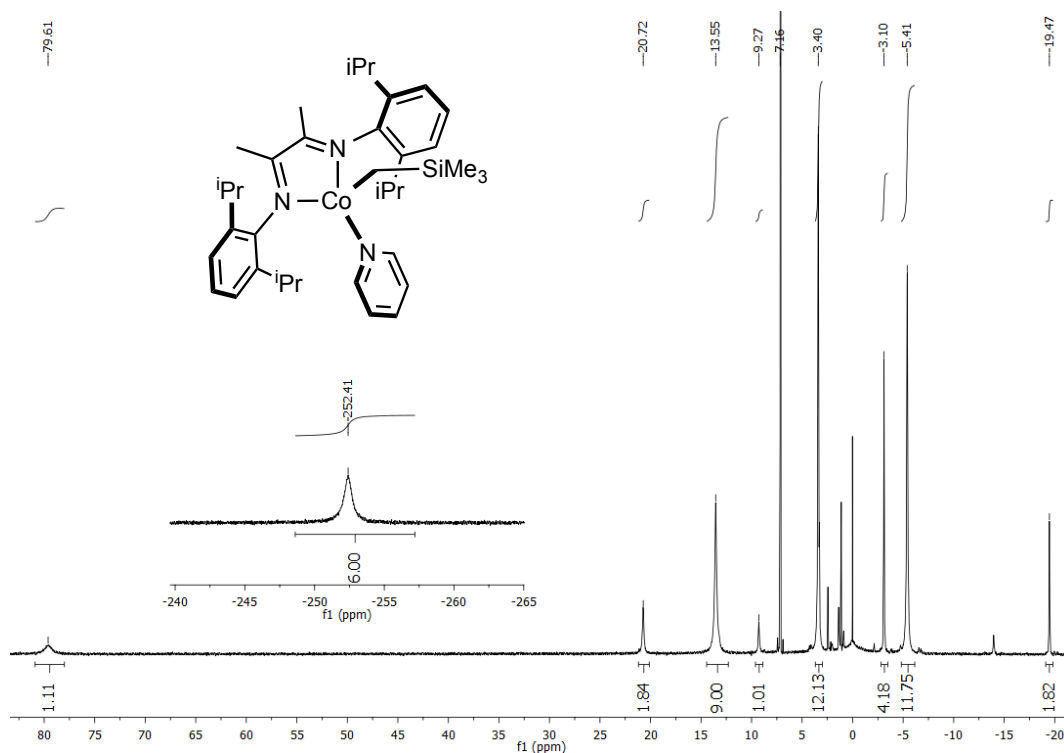


Figure S10. ¹H NMR spectrum (300 MHz, C₆D₆, 23 °C) of **3**. Diethyl ether, SiMe₄, and other trace, residual organic solvents were also observed in the region between 0 and 5 ppm.

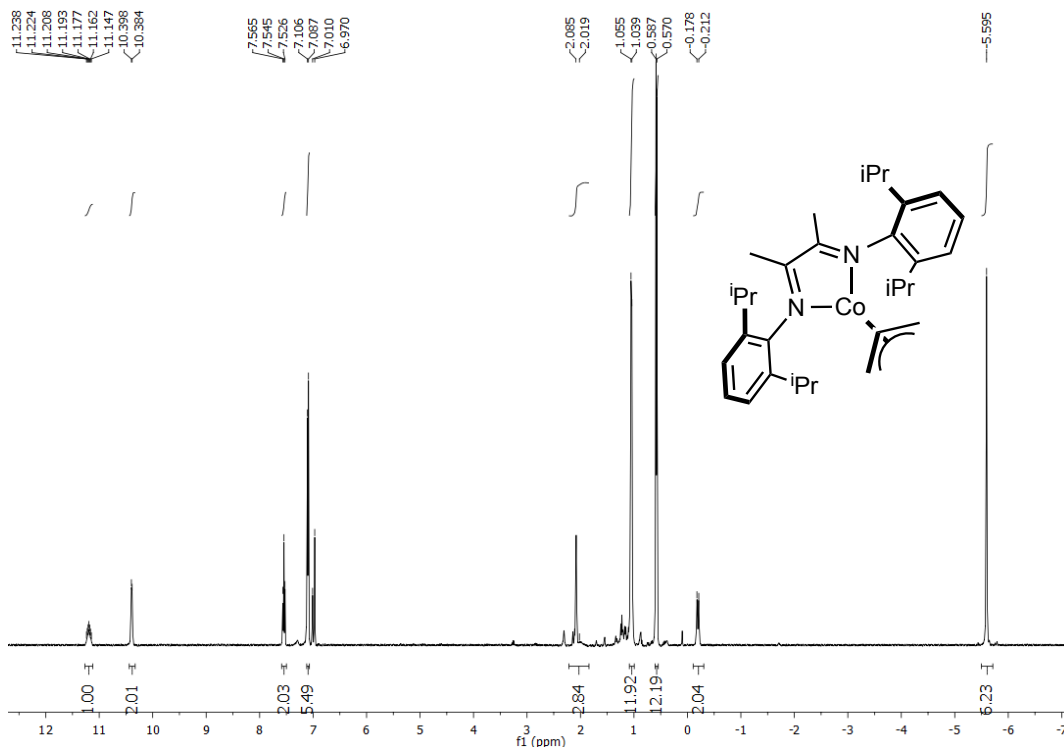


Figure S11. ¹H NMR spectrum (400 MHz, toluene-*d*₈, 21.7 °C) of **4**. Tetramethylsilane, and other trace, residual organic solvents were also observed in the region between 0 and 5 ppm.

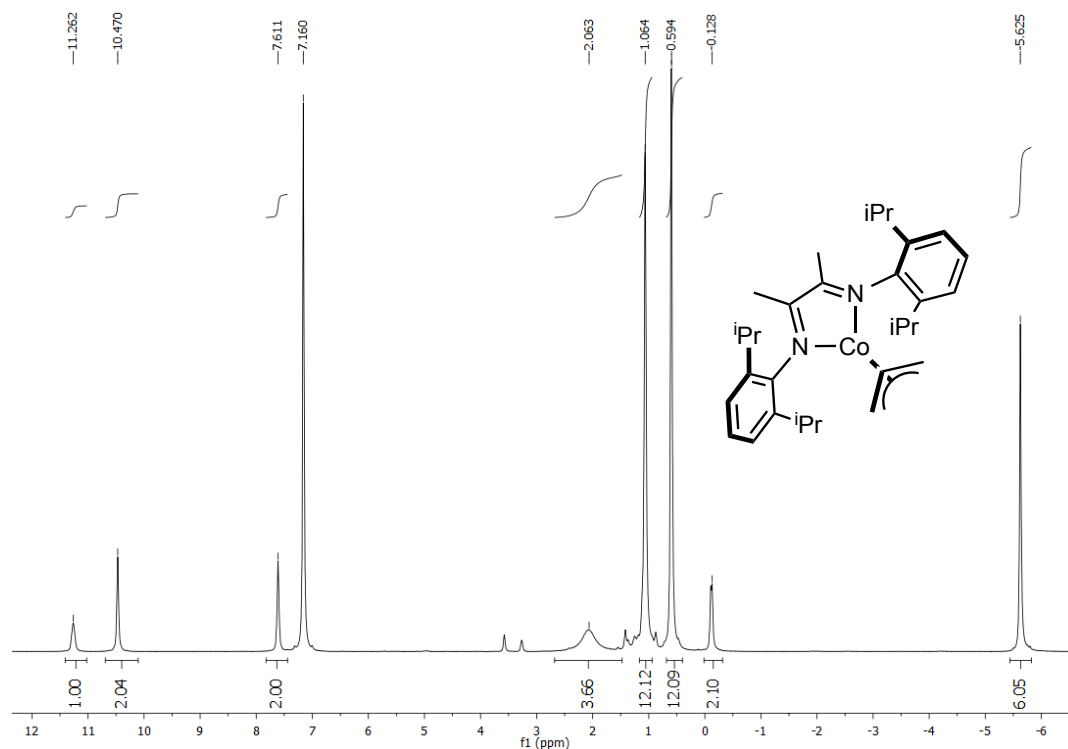


Figure S12. ^1H NMR spectrum (500 MHz, benzene- d_6 , 23 $^\circ\text{C}$) of **4**. Tetramethylsilane, and other trace, residual organic solvents were also observed in the region between 0 and 5 ppm.

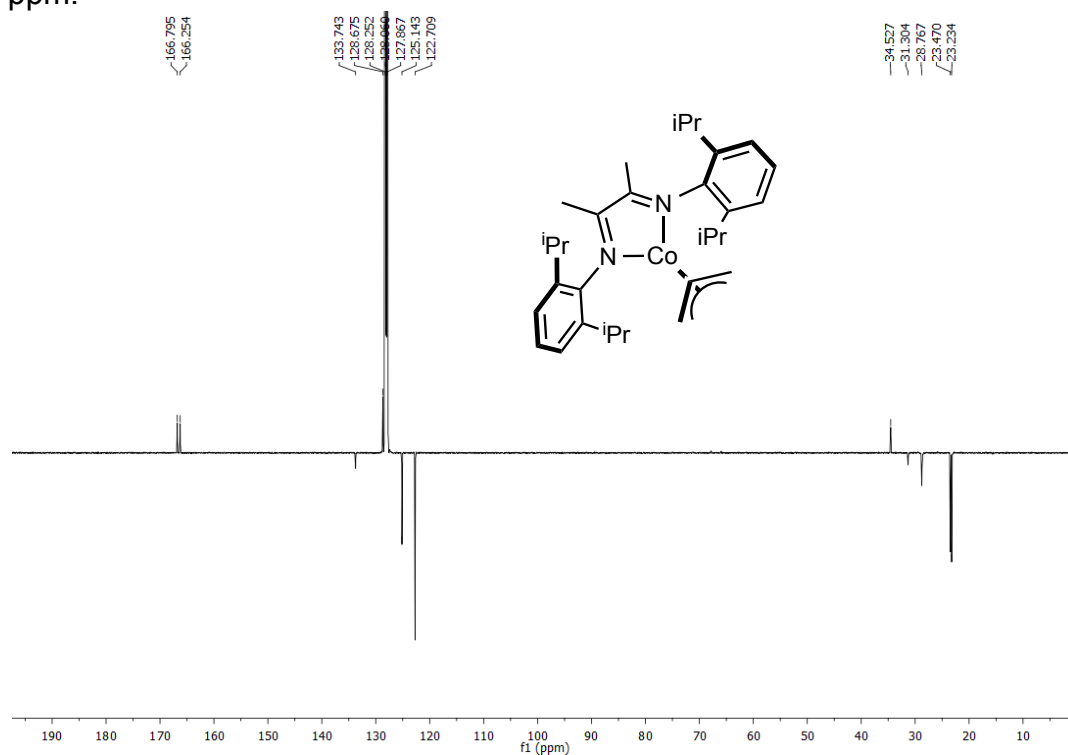


Figure S13. ^{13}C (APT) NMR spectrum (126 MHz, benzene- d_6 , 23 $^\circ\text{C}$) of **4**.

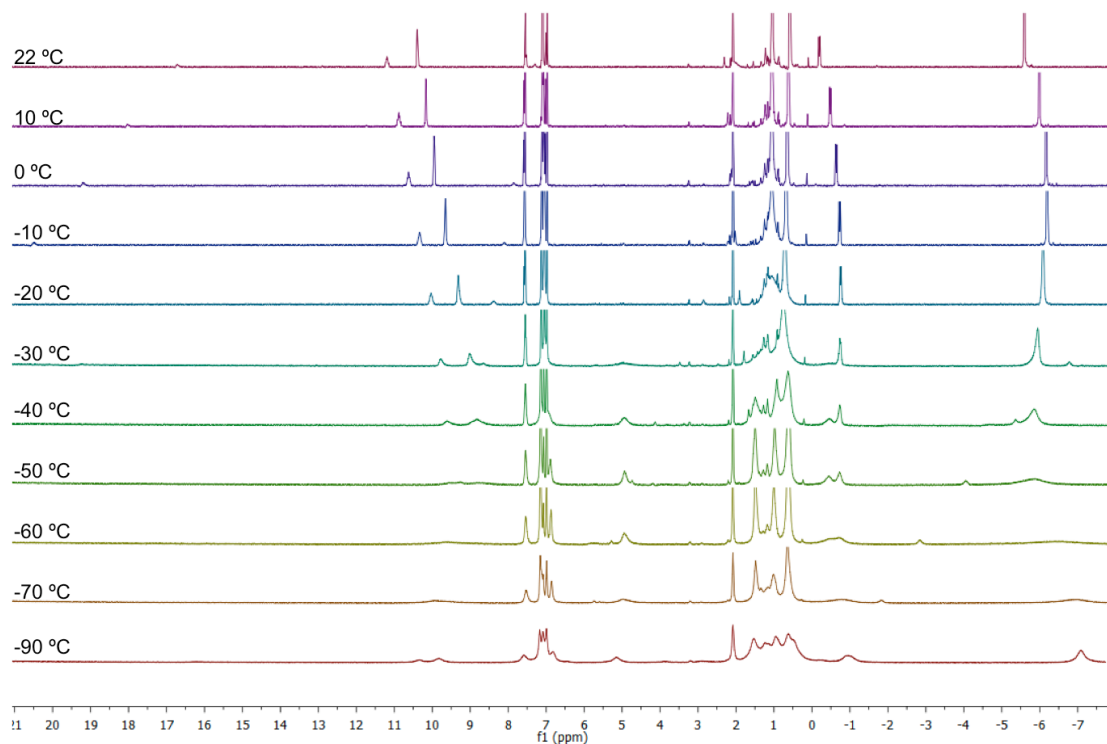


Figure S14. Variable temperature ^1H NMR spectra (400 MHz, toluene- d_8) of **4**.

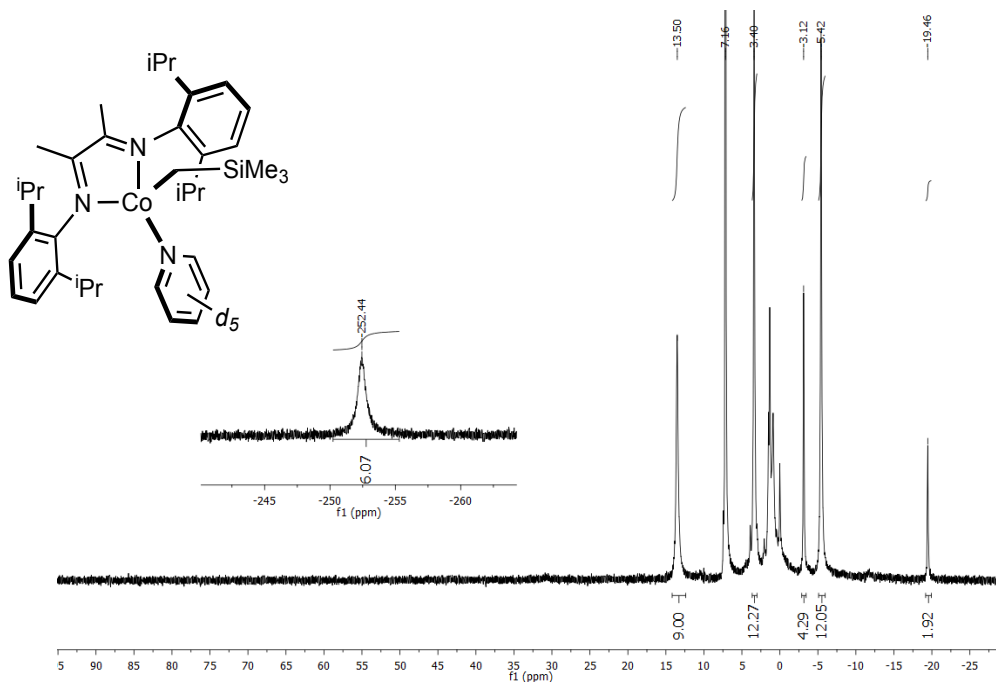


Figure S15. ^1H NMR spectrum (300 MHz, benzene- d_6 , 23 °C) of **3- d_5** .

Tetramethylsilane, and other trace, residual organic solvents were also observed in the region between 0 and 5 ppm.

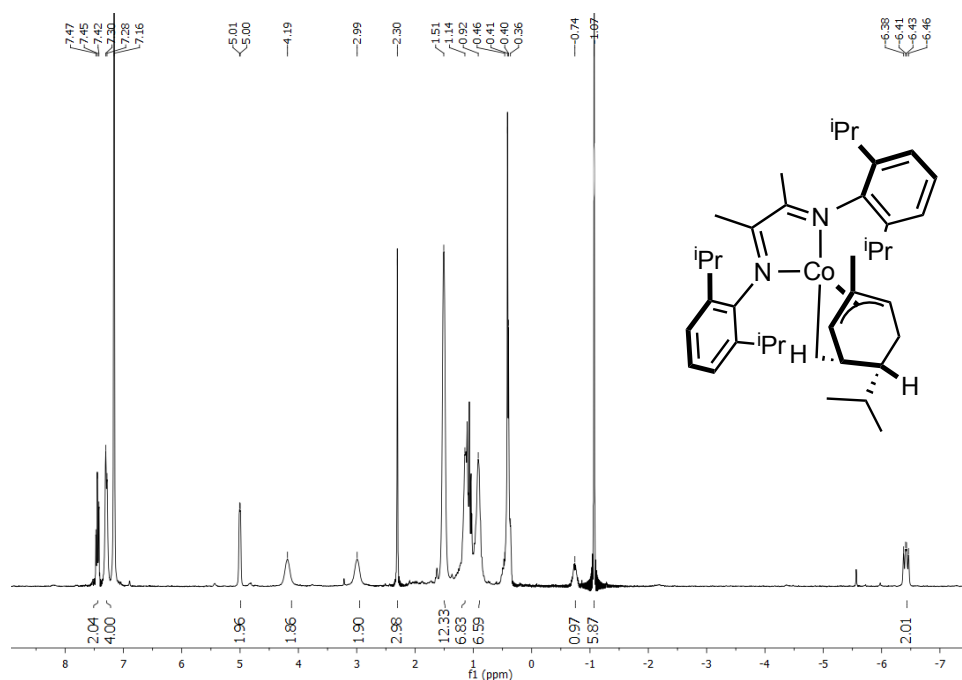


Figure S16. ^1H NMR spectrum (500 MHz, benzene- d_6 , 23 °C) of **5**. Trace residual organic solvents were also observed in the region between 0 and 5 ppm.

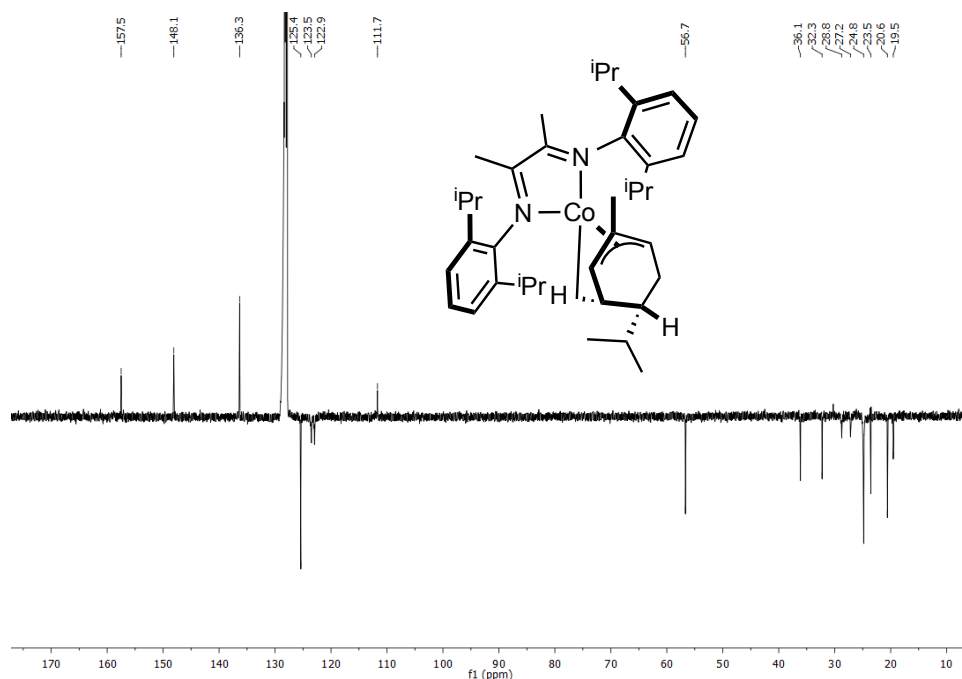
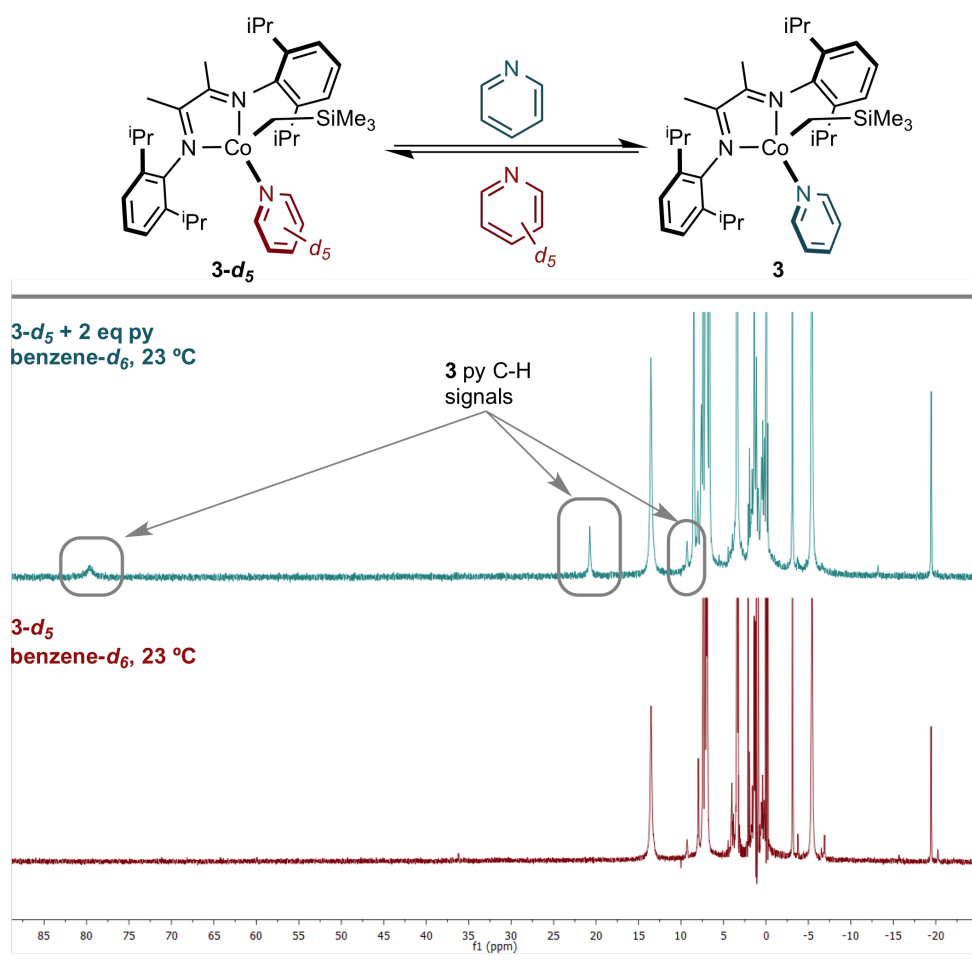
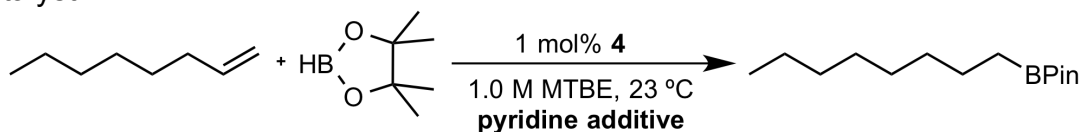


Figure S17. ^{13}C (APT) NMR spectrum (126 MHz, benzene- d_6 , 23 °C) of **5**.



Scheme S1. Pyridine exchange between **3-d5** and **3**. ^1H NMR (300 MHz, benzene- d_6 , 23 °C) spectra show a solution of **3-d5** before (bottom) and 90 minutes after addition of two equivalents of pyridine (top).

Table S11. Pyridine inhibition of the catalytic hydroboration of 1-octene using **4** as a precatalyst.



mol% pyridine	time to completion ^a
0%	<5 min (91%)
5%	6 h (84%)
10%	9 h (80%)
25%	18 h (80%)
50%	18 h (80%)

a) time required to reach >98% conversion, determined by GC-FID analysis. Isolated yields are given in parentheses.

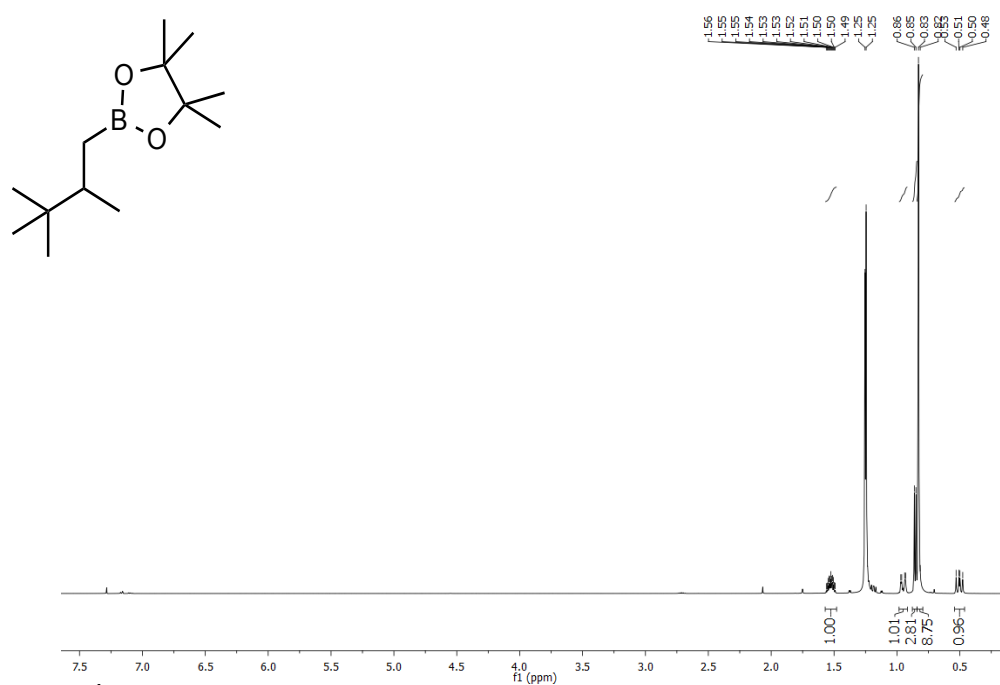


Figure S18. ¹H NMR spectrum (500 MHz, chloroform-*d*, 23 °C) of I.

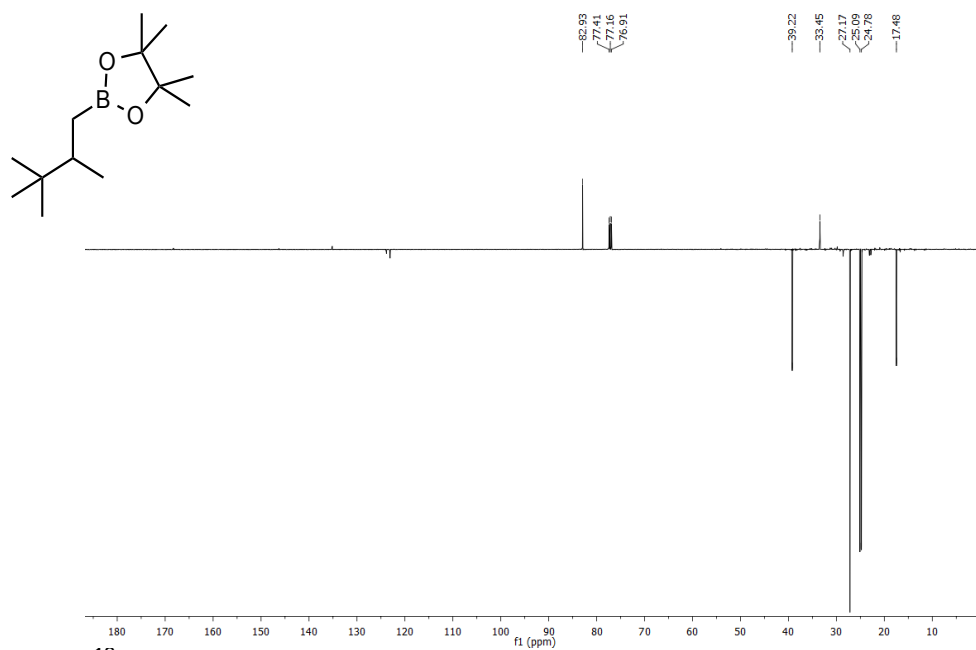


Figure S19. ¹³C (APT) NMR spectrum (126 MHz, chloroform-*d*, 23 °C) of I.

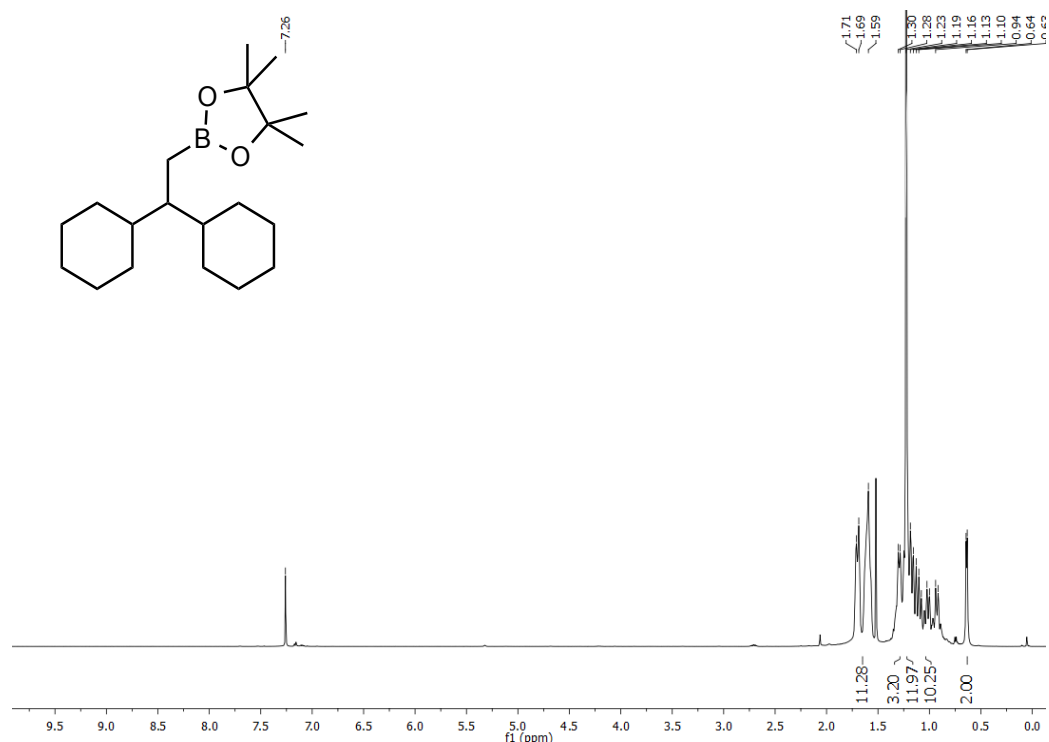


Figure S20 ¹H NMR spectrum (500 MHz, chloroform-*d*, 23 °C) of K.

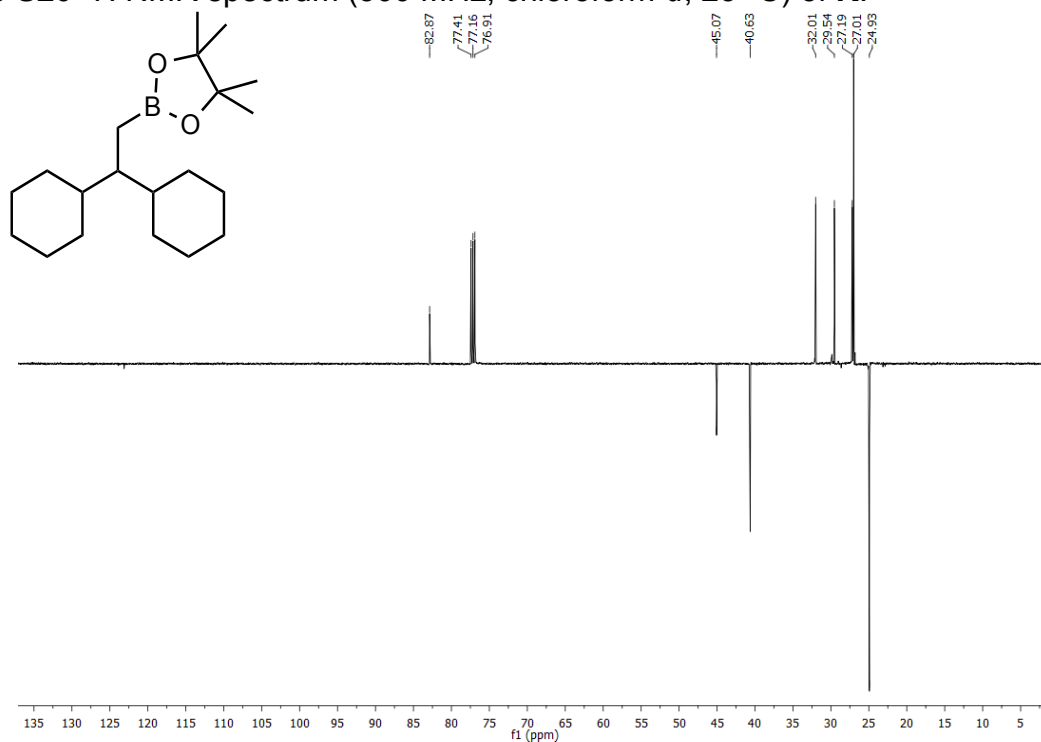


Figure S21. ¹³C (APT) NMR spectrum (126 MHz, chloroform-*d*, 23 °C) of K.

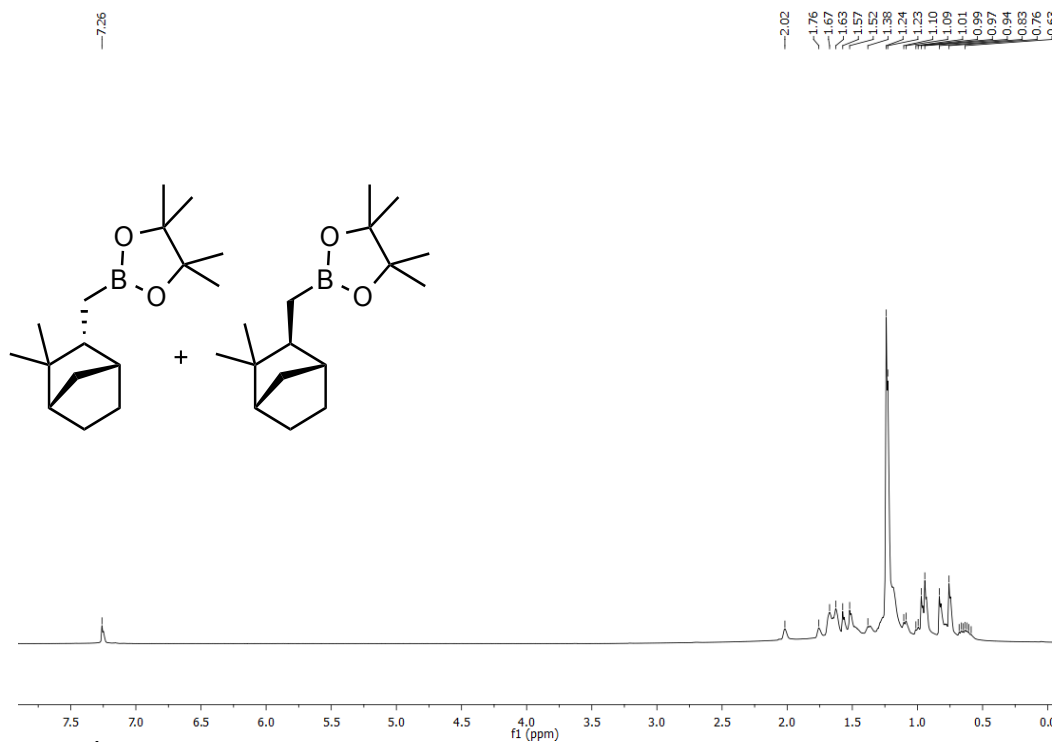


Figure S22. ^1H NMR spectrum (500 MHz, chloroform- d , 23 $^\circ\text{C}$) of L-i + L-ii..

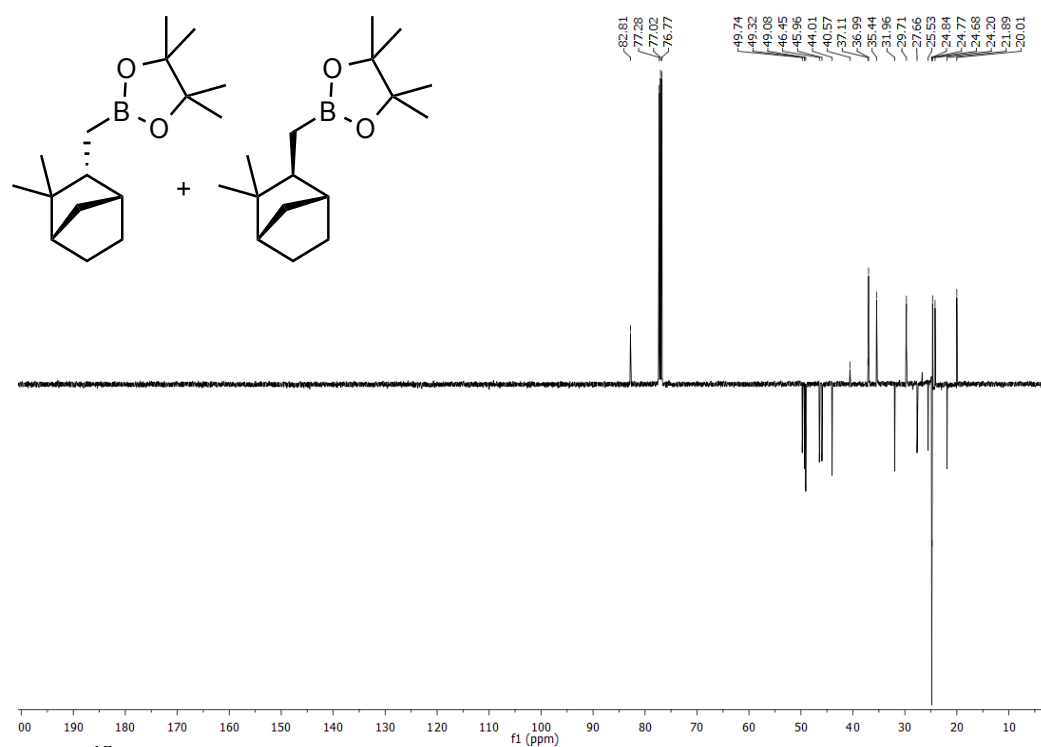
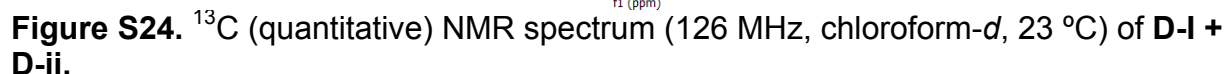


Figure S23. ^{13}C (APT) NMR spectrum (126 MHz, chloroform- d , 23 $^\circ\text{C}$) of L-i + L-ii.



[1] Pangborn, A. B.; Giardello, M. A.; Grubbs, R. H.; Rosen, R. K.; Timmers, F. J. *Organometallics* **1996**, *15*, 1518-1520.

[2] Obligacion, J. V.; Chirik, P. J. *J. Am. Chem. Soc.* **2013**, *135*, 19107-19110.

[3] (a) Bhadbhade, M.; Clentsmith, G. K. B.; Field, L. D. *Organometallics* **2010**, *29*, 6509-6517. (b) tom Dieck, H.; Svoboda, M.; Greiser, T. Z. *Naturforsch., B: Chem. Sci.* **1981**, *36*, 823-832.

[4] Zhu, D.; Janssen, F. F. B. J.; Budzelaar, P. H. M. *Organometallics* **2010**, *29*, 1897-1908.

[5] Young, P. C.; Hadfield, M. S.; Arrowsmith, L.; Macleod, K. M.; Mudd, R. J.; Jordan-Hore, J. A.; Lee, A.-L. *Org. Lett.* **2012**, *14*, 898-901.

[6] Wrackmeyer, B. *Prog. Nucl. Magn. Reson. Spectrosc.* **1979**, *12*, 227-259.

[7] Neese, F. *WIREs Comput Mol Sci* **2011**, *2*, 73-78.

- [8] (a) Becke, A. D. *J. Chem. Phys.* **1986**, *84*, 4524–4529. (b) Becke, A. D. *J. Chem. Phys.* **1993**, *98*, 5648–5652. (c) Lee, C. T.; Yang, W. T.; Parr, R. G. *Phys. Rev. B.* **1998**, *37*, 785-789.
- [9] (a) Schäfer, A.; Horn, H.; Ahlrichs, R. *J. Chem. Phys.* **1992**, *97*, 2571-2577. (b) Schäfer, A.; Huber, C.; Ahlrichs, R. *J. Chem. Phys.* **1994**, *100*, 5829-5835. (c) Weigend, F.; Ahlrichs, R. *Phys. Chem. Chem. Phys.* **2005**, *7*, 3297-3305.
- [10] (a) Eichkorn, K.; Weigend, F.; Treutler, O.; Ahlrichs, R. *Theor. Chem. Acc.* **1997**, *97*, 119-124. (b) Eichkorn, K.; Treutler, O.; Öhm, H.; Häser, M.; Ahlrichs, R. *Chem. Phys. Lett.* **1995**, *240*, 283-290. (c) Eichkorn, K.; Treutler, O.; Öhm, H.; Häser, M.; Ahlrichs, R. *Chem. Phys. Lett.* **1995**, *242*, 652-660.
- [11] (a) Neese, F.; Wennmohs, F.; Hansen, A.; Becker, U. *Chem. Phys.* **2009**, *356*, 98-109. (b) Kossmann, S.; Neese, F. *Chem. Phys. Lett.* **2009**, *481*, 240-243. (c) Neese, F. *J. Comput. Chem.* **2003**, *24*, 1740-1747.
- [12] Ginsberg, A. P. *J. Am. Chem. Soc.* **1980**, *102*, 111-117.
- [13] Noodleman, L.; Peng, C. Y.; Case, D. A.; Mouesca, J. M. *Coord. Chem. Rev.* **1995**, *144*, 199-244.
- [14] Kirchner, B.; Wennmohs, F.; Ye, S.; Neese, F. *Curr. Opin. Chem. Biol.* **2007**, *11*, 134-141.
- [15] Neese, F. *J. Phys. Chem. Solids* **2004**, *65*, 781-785.
- [16] Pettersen, E. F.; Goddard, T. D.; Huang, C. C.; Couch, G. S.; Greenblatt, D. M.; Meng, E. C.; Ferrin, T. E. *J Comput Chem* **2004**, *25*, 1605-1612.
- [17] Yang, X.-J.; Fan, X.; Zhao, Y.; Wang, X.; Liu, B.; Su, J.-H.; Dong, Q.; Xu, M.; Wu, B. *Organometallics* **2013**, *32*, 6945-6949.
- [18] Ganić, A.; Pfaltz, A. *Chem. Eur. J.* **2012**, *18*, 6724-6728.
- [19] Zhang, L.; Peng, D.; Leng, X.; Huang, Z. *Angew. Chem. Int. Ed.* **2013**, *52* (13), 3676-3680.
- [20] Atack, T. C.; Lecker, R. M.; Cook, S. P. *J. Am. Chem. Soc.* **2014**, *136*, 9521-9523.
- [21] Mazet, C.; Gérard, D. *Chem. Commun.* **2011**, *47*, 298-300.
- [22] For a general method of oxidation of pinacolboronate esters with H₂O₂, see: Wu, J. Y.; Moreau, B.; Ritter, T. *J. Am. Chem. Soc.* **2009**, *131*, 12915-12917.

[23] Beckmann, J.; Dakternieks, D.; Duthie, A.; Floate, S. L.; Foitzik, R. C.; Schiesser, C. H. *J. Organomet. Chem.* **2004**, 689, 909-916.